

A REVIEW OF AERONAUTICAL FATIGUE INVESTIGATIONS IN SWEDEN DURING THE PERIOD JUNE 2005 TO APRIL 2007

EDITED by HANS ANSELL

**Saab Aerosystems
Sweden**

ICAF Doc. No. 2411



CONTENTS

3.1	INTRODUCTION	3
3.1.1	Saab 70 years 1937-2007	3
3.2	ACCIDENT INVESTIGATION	4
3.2.1	Accident with a CASA C-212 aircraft during maritime patrol operation.....	4
3.3	STRUCTURAL EVALUATION	7
3.3.1	The Saab 2000 Full Scale Fatigue Test and Damage tolerance Test.....	7
3.3.2	Empennage structure, fatigue and damage tolerance test.....	7
3.3.3	Wing/fuselage fatigue test.....	9
3.3.4	Engine Mount structure fatigue test.....	11
3.3.5	JAS39 Gripen Fatigue Testing	12
3.3.6	Full scale fatigue test of the single seater, 39A	12
3.3.7	Full scale fatigue test of the twin seater export version, 39D.....	13
3.3.8	Export Standard Pylons Fatigue Tests	15
3.3.9	Refuelling Transfer Units Fatigue Tests	17
3.4	FATIGUE CRACK INITIATION AND PROPAGATION	20
3.4.1	Crack growth simulation for stiffened panels.....	20
3.4.2	Stochastic evaluations of fatigue crack initiation and propagation	22
3.4.3	Towards large scale simulations of multiple site fatigue damages	23
3.4.4	Crack propagation in welds.....	25
3.4.5	A modification to the Neuber rule	27
3.4.6	Critical plane method for crack initiation analysis	28
3.4.7	Reliability based life prediction.....	29
3.4.8	Fatigue testing of metal laminate coupons	31
3.5	COMPOSITE MATERIALS.....	33
3.5.1	Delamination fatigue modelling and constant mode fatigue behaviour	33
	ACKNOWLEDGEMENTS	38

3.1 INTRODUCTION

In this paper a review is given of the work carried out in Sweden in the area of aeronautical fatigue during the period June 2005 to May 2007. The review includes basic studies of fatigue development in metals and composites, stress analysis and fracture mechanics, studies of crack initiation and propagation and residual strength, testing of full-scale structures, and fatigue life predictions. A reference list of relevant papers issued during the period covered by the review is included.

Contributions to the present review are from the following bodies:

- The Swedish Defence Research Agency (FOI), Aeronautics Division, FFA
Sections 3.4.1, 3.4.2, and 3.4.3
- SAAB Aerosystems
Sections 3.3.1, 3.3.2, 3.3.3, 3.3.4, 3.3.5, 3.3.6, 3.3.7, 3.3.8 and 3.3.9
- VOLVO Aero Corporation
Sections 3.4.4, 3.4.5, 3.4.6, and 3.4.7
- The Swedish Accident Investigation Board (SHK)
Sections 3.2.1
- The Swedish Institute for Composites (SICOMP)
Sections 3.5.1
- Linköping University (LiU)
Sections 3.4.8

3.1.1 Saab 70 years 1937-2007

The year 2007 marks the 70th anniversary of Saab – Svenska Aeroplan Aktiebolaget. It was founded on April 26, 1937 to supply the state of Sweden with domestic aircraft in time of war - to defend and guard Sweden's long international border. Since that time Saab has been a successful aircraft manufacturer and supplier of defence materiel and more than 4000 aircraft have been built ever since. The company still acts under the name Saab and has developed into an international defence company consisting of several brances but will always remain as a part of Swedish industrial history.



Figure 1. Saab aircraft

3.2 ACCIDENT INVESTIGATIONS

3.2.1 Accident with a CASA C-212 aircraft during maritime patrol operation.

On October 26, 2006, a CASA C-212-CE aircraft operated by the Swedish Coast Guard in a maritime patrol role had a fatal accident. During a low by-pass over the harbour bay the aircraft suddenly lost control after separation of the left side wing and crashed into the sea. A full investigation, conducted by the Swedish Accident Investigation Board, was immediately initiated.

Examination of the aircraft exposed a structural failure at the centre wing close to the fuselage, figure 2.



Figure 2. CASA-212-CE aircraft in maritime patrol operation.

After initial examination of the evidences, cracks, suspected to be caused by fatigue, were found in the centre wing lower skin at STA Y=1030. The lower wing skin at this station has an external doubler riveted to wing skin consisting of 6 rivet rows. The cracks were confined to the first rivet row in the skin where the external doubler ends. At the cracked row, there is also a fairing connecting the wing to the fuselage aimed to carry horizontal loads in the aircraft longitudinal direction. The design of this fairing is however also supposed to transfer some vertical loads which partly may have contributed to the cracking by induced bending in the failed section. Fatigue cracked rivets give evidence of such an assumption.

The cracking was wide spread extending over a large portion of the wing chord, figure 3. Figures 4 and 5 details the cracks through the wing skin at fastener holes and at locations between the holes. The cracks between the holes seem to follow scratches and marks possibly originating from skin machining operations. Cracks were also found in the same area of the right hand side wing, figure 6. At the time of the accident, the aircraft had accumulated 17,000 flight hours and 7,300 flight cycles.

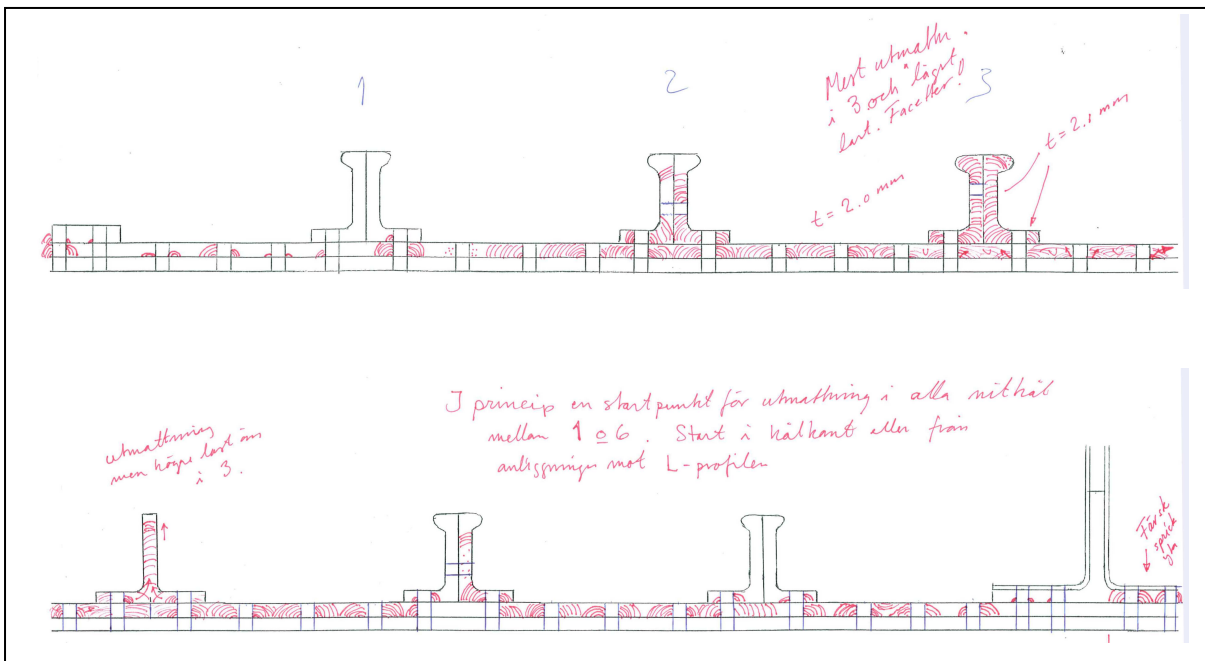


Figure 3. Schematic fatigue crack pattern in the left wing skin at STA Y=1030.

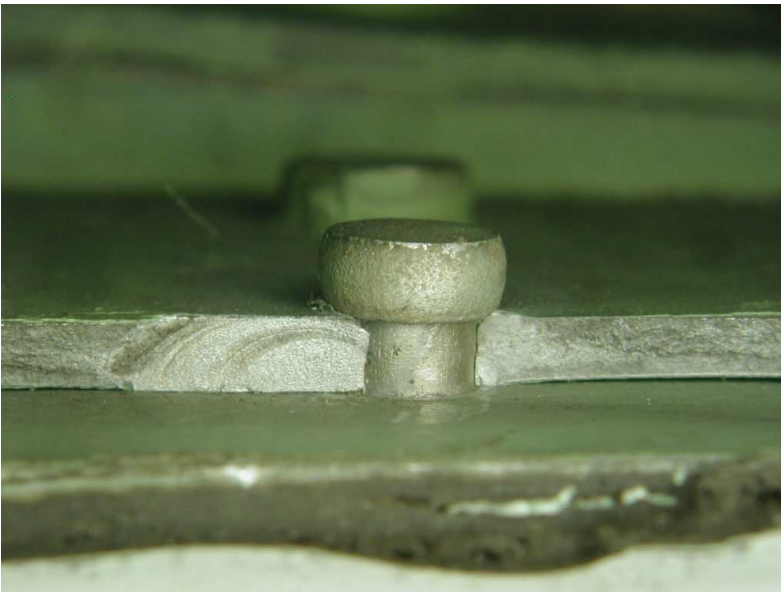


Figure 4. Evidence of fatigue crack initiation at rivet holes, left wing.

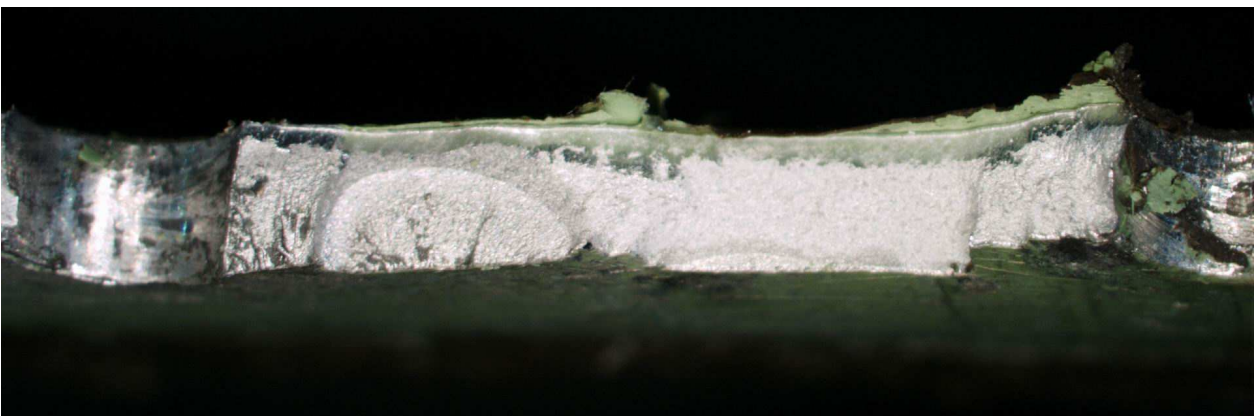


Figure 5. Evidence of fatigue crack initiation between rivet holes, left wing.

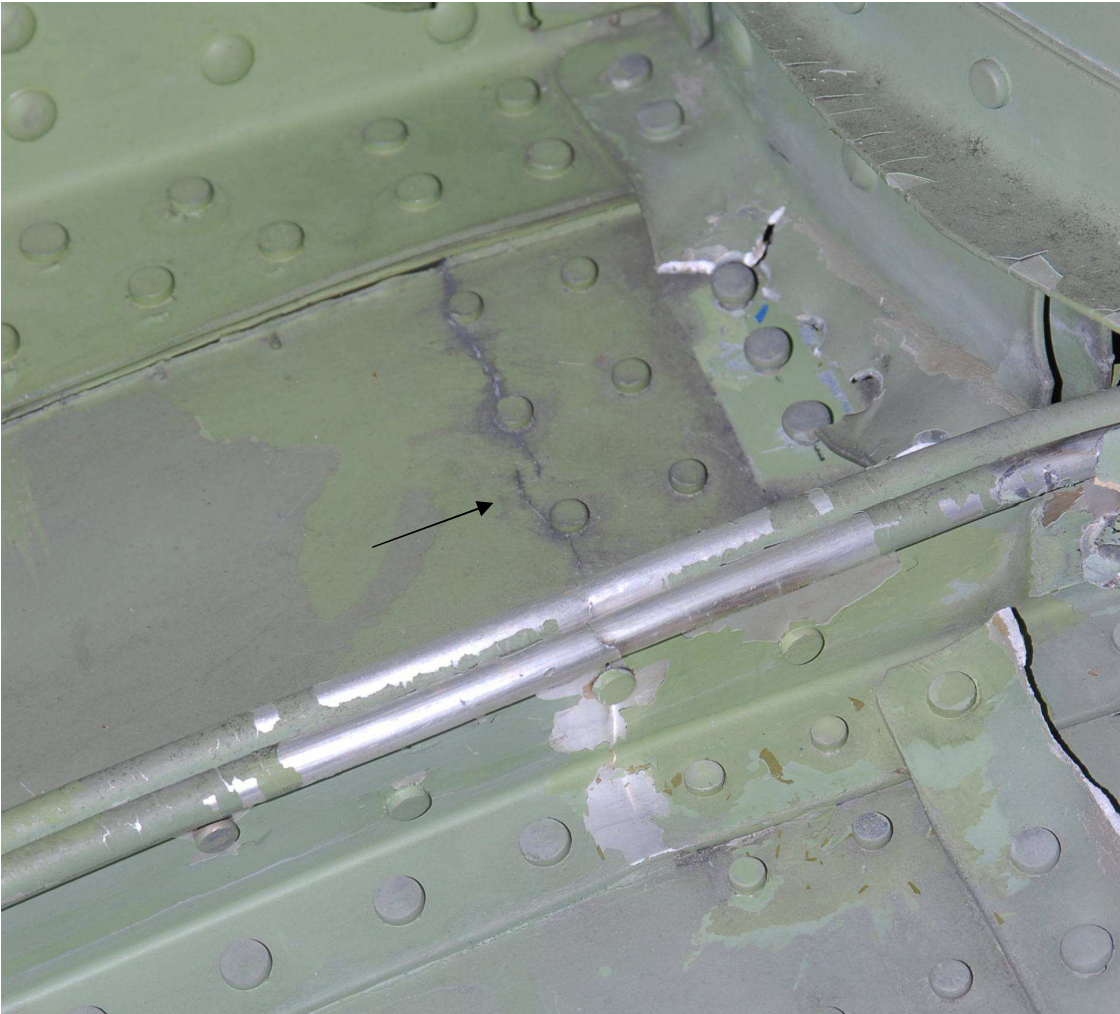


Figure 6. Multiple fatigue cracking in the right wing.

The investigation of the cause of the accident is ongoing in close cooperation with consultants to the Swedish Accident Investigation board and the Spanish aircraft manufacturer CASA. Several specific investigations are carried out:

- Inspection for cracks in other C-212 aircraft. At this point no cracks have been found in this area in any other aircraft.
- Investigation of the operation of the aircraft type in maritime patrol service and in similar low altitude operations. The mission mix and profiles in Search and Rescue operation is under investigation.
- Investigations into possible sources of vibration.
- Fractographic and other metallurgical investigations.
- A complete structural test program with coupons and panels with all the parameters which could have had an influence on crack initiation (type of rivet, sealant, scratches, fairing induced load, etc.).
- A flight test program to measure the loads introduced by the wing-fuselage fairing.

3.3 STRUCTURAL EVALUATION

3.3.1 The Saab 2000 Full Scale Fatigue Test and Damage tolerance Test

The Design Service Goal (DSG) for Saab 2000 is presently 75000 flights or 60000 flight hours whichever occurs first. For the Saab 2000, no complete airframe will be tested due to the commonality with the Saab 340. Consequently, a number of full scale component tests are used to justify the long term characteristics.

3.3.2 Empennage structure, fatigue and damage tolerance test

This test included the horizontal stabilisers and the attachment structure to the rear fuselage. The fatigue phase including the damage tolerance test is completed, comprising of 150000 flights in pure fatigue test with subsequent testing with artificial notches for further 24000 flights.

A total number of four artificial damages were inflicted on the test specimen. These artificial damages can be classified into two types as follows:

- Damages where the intention is to study the crack growth rate.
- Damages in fail safe structure, where the primary load path is removed. In this case the "residual fatigue life" of the remaining load paths, i.e. the time to initiation of secondary cracks, is of interest. The subsequent crack growth rate of possible secondary cracks will also be studied.

The following structural elements of the horizontal stabiliser have been subjected to artificial cracks. This was made by mechanical means in terms of sawing, grinding or cutting.

- Stabiliser/fuselage attachment
Study of crack growth rate for a crack in the stabiliser spar cap, from a fastener hole at the attachment to the fuselage frame.
- Rear spar web
Study of crack growth rate for a crack growing from an inspection hole.
- Upper skin panel
Study of crack growth rate for a crack growing from a fastener hole towards the honey comb core.
- Mid hinge
Study of crack growth rate for a crack growing from a fastener hole (LHS), study of residual fatigue life and crack growth of possible secondary cracks after complete failure of one of two parts in the mid hinge (RHS).

The rationale for selecting the aforementioned damages is that the damages shall cover relevant types of spectra, crack types and materials in order to constitute a substantiation of the damage tolerance analysis of the Saab 2000 horizontal stabilisers.

The experiences from the damage tolerance testing have been taken into consideration in the damage tolerance verification and if necessary the existing in service inspection program has been updated to reflect the results from the testing.

Residual strength tests have taken place to show compliance with the FAR/EASA requirements with respect to residual strength evaluation. This implies that the remaining structure must be able to withstand an arbitrary limit load condition.

The horizontal stabilizer was tested with four critical artificial saw cuts located at the most critical location of the principal structural elements. Primary spars, critical sections of the panel and attachment to fuselage were provided artificial saw cuts corresponding to critical sizes per the theoretical analysis. Figure 6 outlines the artificial saw cut at the inboard section where the main spar is attached to the fuselage frame.

The residual static tests were carried out up to at least limit load level with satisfactory results. Based on these results, it was thereby demonstrated that the empennage structure to the Saab 2000 fulfil all civil requirements (FAR/EASA regulations) of residual strength capability.

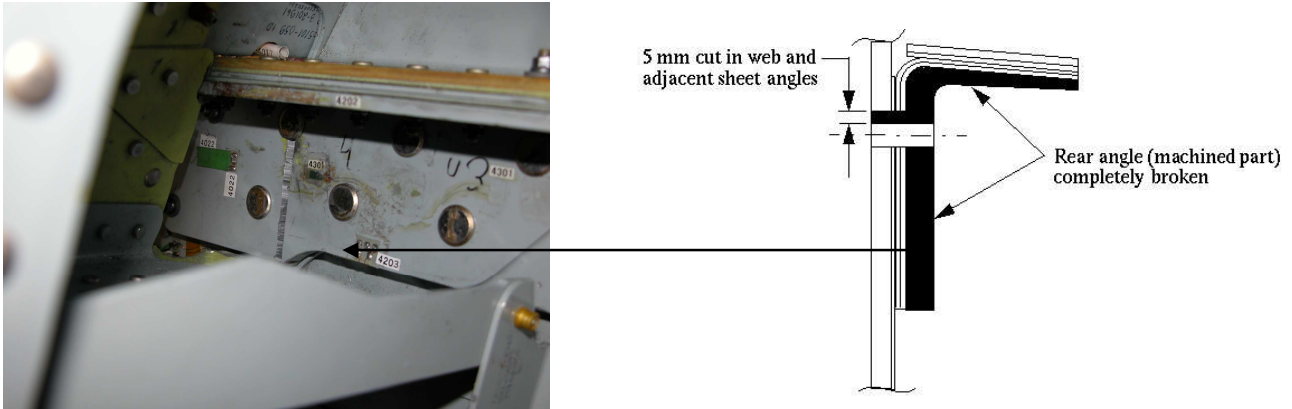


Figure 6. Saab 2000 Residual strength test- artificial saw cut at the inboard section of the horizontal stabilizer

Subsequently, accidental damages in terms of multiple and major dents were also tested during a separate residual strength test. All saw cuts except the saw cut at the inboard section were repaired prior to this final test. The lower skin panel was provided with multiple dents simulating inappropriate maintenance on aircraft in service. Figure 7 depicts the distribution of the multiple dents in the panel. The test specimen was loaded to 178 % of the limit load level before test was interrupted due to limitations in the loading system. The test specimen maintained the structural integrity at this high load level, no discrepancies were noted in the spar interface or at zone for the artificial dents per figure 7.

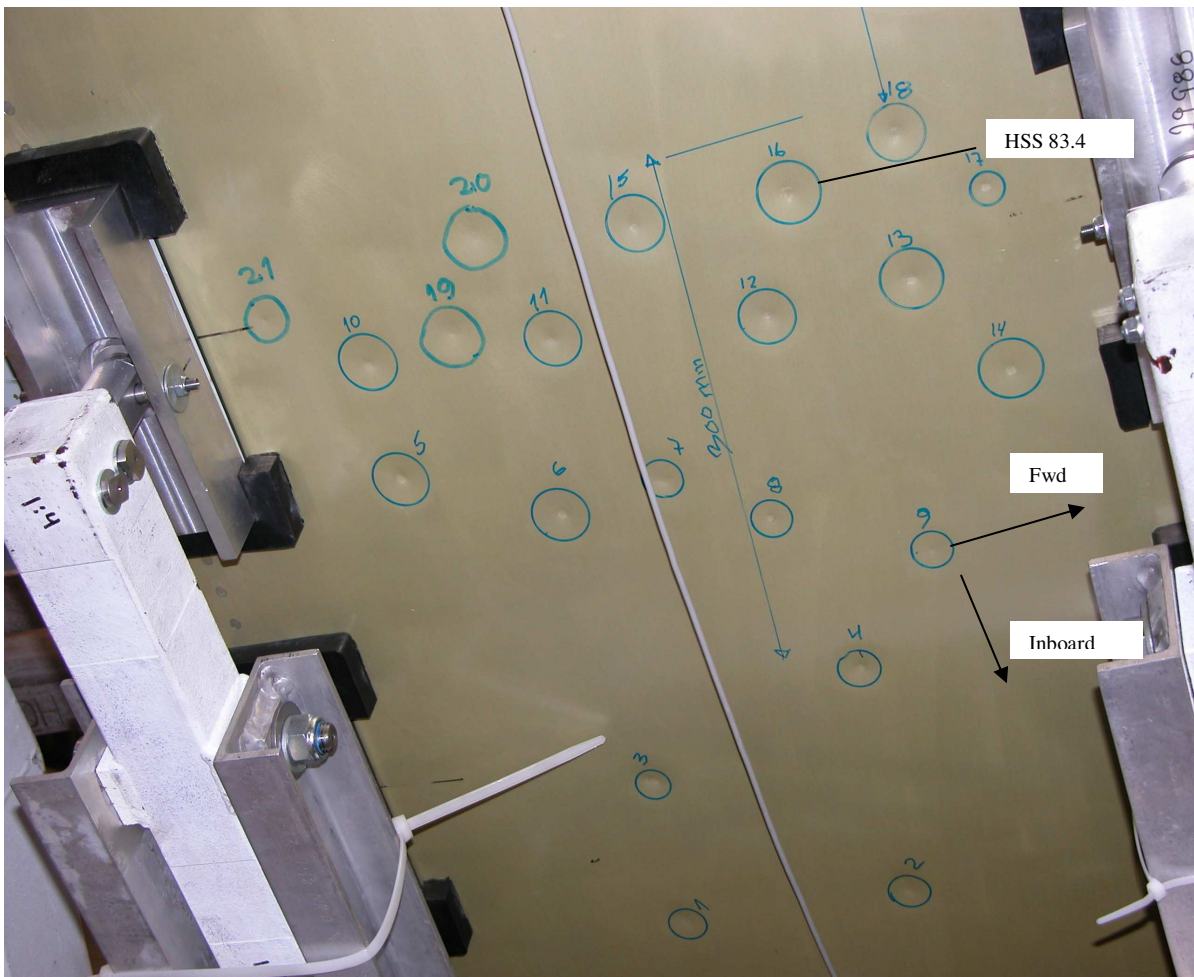


Figure 7. Saab 2000 Residual strength test- 178 % limit load level simulating accidental damages

3.3.3 Wing/fuselage fatigue test

The subject test includes the centre and the rear part of the fuselage, the complete wing torque box and the rear part of the engine nacelles.

The wing detail design is changed compared to the Saab 340 (machined spars with integral spar caps), and the wing/fuselage interface also. Furthermore the cabin pressurisation spectrum is more severe, more exactly twice as severe as the spectra for the Saab 340 aircraft. The flight and landing loads on the fuselage is also more severe due to the slender fuselage of Saab 2000.

The first part of Wing/Fuselage Fatigue test up to 150000 flights with fatigue loads is finalised. Subsequently, the damage tolerance testing will continue aiming to reach 2'12000 flights with artificial notches. Twenty six different types of damages have been defined reflecting the damage tolerance characteristics of various principal structural elements of the Saab 2000 airframe.

In conformity with other tests, the wing/fuselage structure will be tested to demonstrate the damage tolerance characteristics in accordance with airworthiness requirements specified in FAR/EASA regulations. This also includes residual strength tests up to limit load condition for selected and critical load cases.

Since a limited no of damages shall represent damage tolerance characteristics of all critical parts, a careful selection has been carried out.

The criteria for selecting which damages to test have been:

- Damages with impact on flight safety
- Damages with short calculated total crack growth life
- Damages in fail safe structure, for which the calculated crack growth life after failure of one load path is short
- Damages for which it is desirable to improve the in-service inspections

The selected damages cover different types of structural parts, such as wing panels, wing spars, fuselage panels, reinforced fuselage cut-outs, wing and fuselage splices. They also cover different types of crack origins, such as for example free edges, open holes and holes with pin load.

The selected damages also cover the different materials which are considered to be of interest with the actual sequence.

Figure 8 on the following pages summarizes the location the artificial cracks introduced on the Saab 2000 airframe. Figure 9 depicts an example of introduced artificial cracks on the lower wing panel, the internal located stringer is also simulated to be broken (through cutting of the entire stringer) Figure 10 outlines an artificial crack in the forward lower spar cap including a similar damage to the outer wing skin.

The test sequence used in the damage tolerance phase is the identical to sequence used in the fatigue phase. Thus, this sequence is truncated in terms of reduction of load cycles with small ranges. For damage tolerance testing is also crucial to consider load cycles with small amplitudes or ranges due to the contribution to the total crack propagation. Instead of using a revised test sequence it has been verified that the existing sequence can be adapted with the addition of more test cycles to the previous defined test sequence.

Until today, the damage tolerance test has been tested for 14000 flights without any significant and overall crack propagation. The artificial crack that been propagated is the saw cut including notch on the lower wing skin (depicted in figure 9).

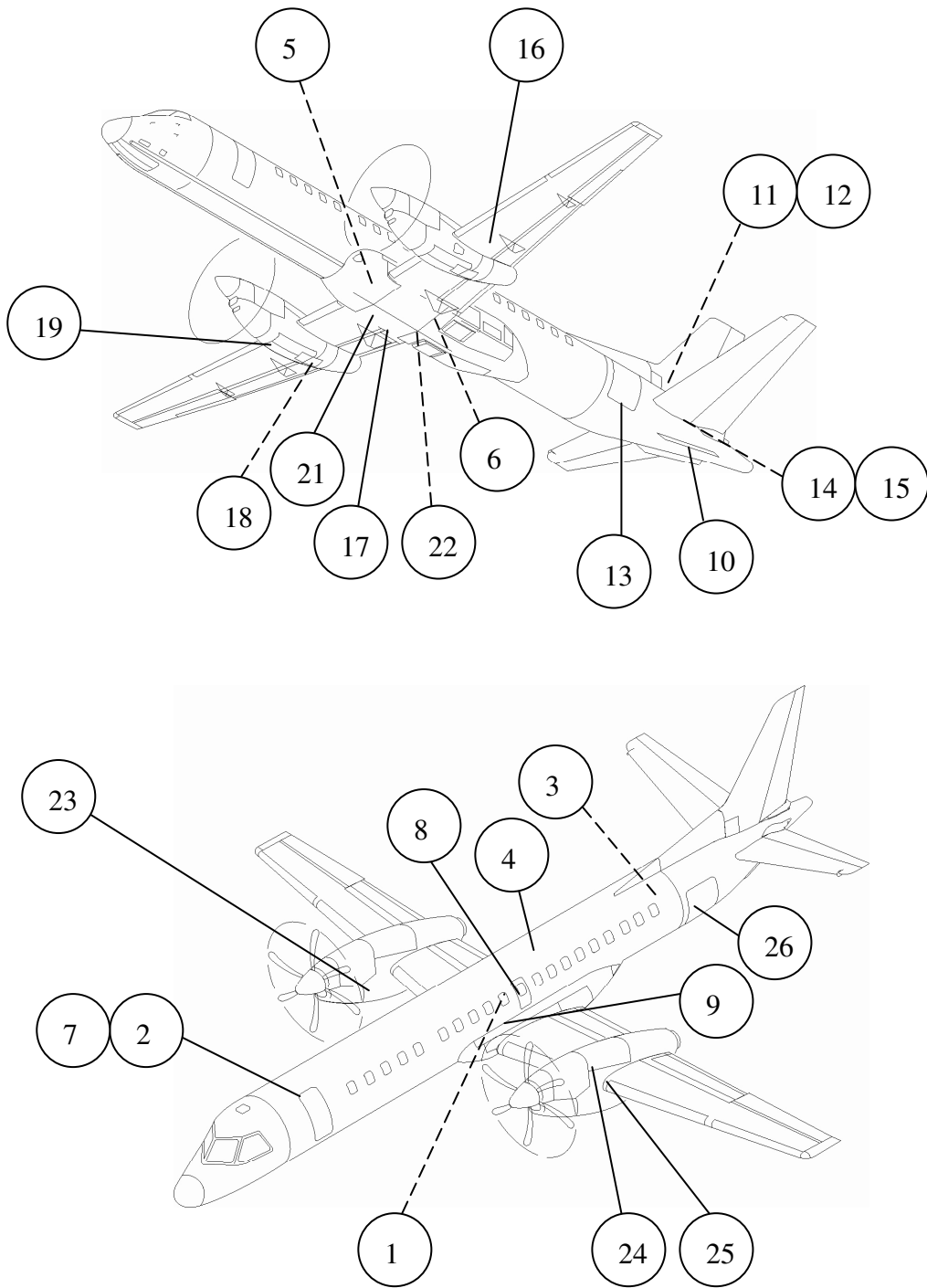


Figure 8. Saab 2000 Overview of all artificial cracks



Figure 9. Saab 2000 Artificial crack in lower wing skin with an broken stringer



Figure 10. Saab 2000 Artificial crack in lower forward wing spar cap and in skin

3.3.4 Engine Mount structure fatigue test

The Saab 2000 engine mounting structure is completely different in design compared to the Saab 340. Eighth steel struts attaching to the forward engine mounts to the nacelle structure basically build up the structure. Each of those eight struts is redundant in terms of continuing airworthiness if an arbitrary strut is failed.

The fatigue phase of the test is completed (verification of 150000 flights from fatigue point of view). A number of fail safe situations (simulating a broken strut or fitting) with respect to the fatigue behaviour are tested in order to check the fail safe characteristics of the entire trussgrid under the fatigue loading. This portion of the test verified the fail-safe concept for a time period of 3*12000 flights.

The damage tolerance phase with artificial cracks will be final phase of this test programme.

3.3.5 JAS39 Gripen Fatigue Testing

The strength verification programme with large components was completed during 1994. The full scale fatigue test of the twin seater, 39B, was completed in 2000. The full scale fatigue test of the single seater, 39A, is still running in order to verify an extended life of the wing and fin of the C/D versions. The full scale fatigue test of a twin seater export version, 39D, is running.

3.3.6 Full scale fatigue test of the single seater, 39A

The configuration of the major fatigue test is almost identical to that of the major static test, both with regard to the structure and the test arrangement, figure 11. The test set-up has about 90 control channels, more than 1,000 strain gauges installations and is monitored by acoustic emission, besides the inspection by conventional methods.



Figure 11. Photograph of the full scale fatigue test of the Gripen single seater, 39A.

The initial aim to verify a service life of 4,000 hours (5,600 flights) by flight simulation testing to 16,000 hours (22,400 flights) was completed in 1999. No significant cracks were detected during and after the testing except in parts belonging to the air brakes.

The objectives with testing beyond 16,000 hours, with the aim to reach 32,000 hours, are to verify wing and fin structure for the C and D versions of the aircraft. Another secondary goal is to identify areas in the fuselage where fatigue, in the long run, may show up in the A and B versions. The test has today (May 2007) reached the target life of 32,000 hours (44,800 flights). Between 16,000 hours and 32,000 hours a few cracks have been found:

- in a lug for the attachment of the actuator for the main landing gear door.
- at hole edges in webs of formed sheet frames.
- at tool holes in the web of a machined fin attachment frame.
- surface cracks in radius in the root rib of the main wing due to residual stresses from assembly.

The outcome of the test has been used to retrofit operational aircraft and to redesign parts for the C and D versions for the Swedish airforce as well as for export aircraft. The lug for the main landing gear door actuator and the parts for the

airbrake are redesigned. The formed sheet frames are replaced by high speed machined integral frames and the web of the machined fin attachment frame is made thicker. The cracking of the root rib, figure 12, affects only a very few A version aircraft since the wing assembly was changed early in the production. A repair procedure has been designed and verified in the test for these aircraft and can be applied if necessary. The cracking is no flight safety issues but the rectifying actions have been made in order to avoid any cracking at all during the design life.



Figure 12. Surface cracks in radius in the root rib of the main wing due to residual stresses from assembly.

3.3.7 Full scale fatigue test of the twin seater export version, 39D

The test object is a complete fuselage, figure 13 and 14. Attachment loads from the wings, fin, foreplanes, landing gears etc. are applied via dummies. The whole test set-up has about 90 control channels (actuators and pressure valves) and the structure is equipped with more than 1,000 strain gauges.

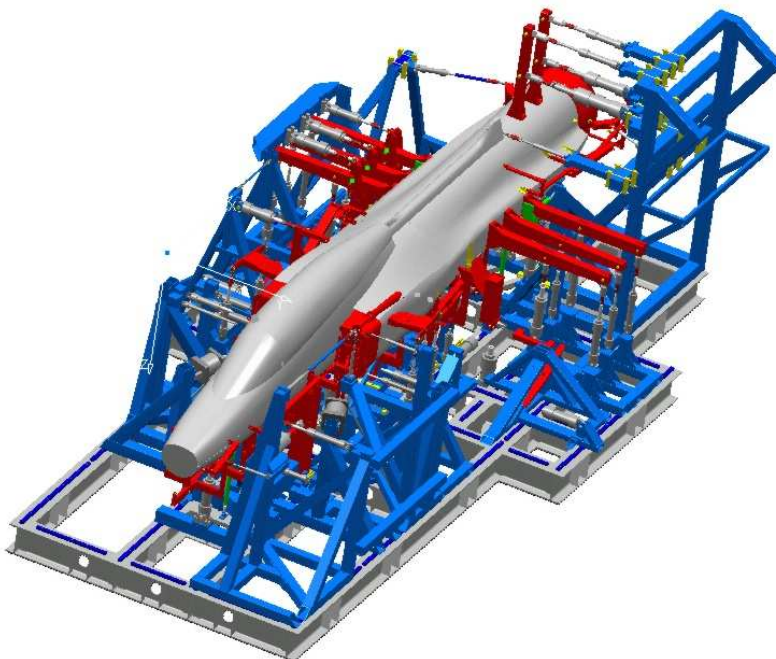


Figure 13. Schematic drawing of the full-scale test of Gripen twin-seater 39D.



Figure 14. Photograph of the forward fuselage, D version, with the air-to-air refuelling probe dummy.

The test is made in order to verify:

- Increased service life (8,000 flh)
- Changes due to part count reduction (e.g. introduction of high speed machined integral parts)
- Changes due to world wide climate adaptation (WWC)
- Increased cabin pressure
- Increased basic design mass
- Changes due to Air-to-Air Refuelling installation (AAR)

A number of unit load cases and balanced load cases have been subjected to the test object before fatigue testing. The measured data have been used to certify new structures for full flight envelope. Some of the load cases will be measured after every 1,000 flight hour block of fatigue testing as well.

The repetition test sequence for the fatigue test consists of about 400 flights representing 500 flight hours. The goal is to exceed 32,000 flight hours of test simulation. The fatigue testing was started in January 2004 and has today (May 2007) reached 21,500 hours. Major inspections were done at 8,000 and 16,000 hours. A few cracks have been found:

- in a lug for the attachment of the actuator for the main landing gear door, figure 15
- in a lug for the attachment of the actuator to the air-brake, figure 16

Improved replacements of cracked parts have been designed and are verified in the on-going test.



Figure 15. Cracked lug for the attachment of the actuator for the main landing gear door



Figure 16. Cracked lug for the attachment of the actuator to the air-brake

3.3.8 Export Standard Pylons Fatigue Tests

The development of weapon pylons, covering both wing and fuselage mounted pylons, compatible for NATO stores for the Gripen fighter was initiated in 1997. Common to all pylons are a box structure design built around a mechanism by which the stores are pre-tensioned to the pylon.

To support static stress analysis, some static tests were performed. Static strength requirements were defined as: no permanent deformation allowed at 100 % limit load and no failure allowed at 150 % limit load.

Failure of outboard wing pylon #2, was reached at 300 % limit load, no permanent sets were observed at 100 % limit load. Analysis predicted failure at 240 - 290 % limit load (friction dependent load paths caused the scatter). The inboard

wing pylon #3 was tested to 225 % limit load without failure with only minor permanent sets at this load level. The off center fuselage mounted pylon #4, reached failure at 300 % limit load, no permanent deformations was detected at 150 % limit load.

The fatigue test rig is identical to the one used for the static tests, figure 17. The test rig set up is similar for all the pylons. The pylons are mounted up side down with a stiff solid beam acting as a dummy store. Air load on the pylon are applied using two cylinders with pads distributing the load to the sideplates. Air and inertia store loads are applied on the dummy store using seven cylinders. Pretension and release of pretension of stores are also simulated in the fatigue test by using an electric torque wrench operated by the test rig control system.

The initial aim of the fatigue test, common to all the pylons, is to verify a safe life of 4000 flight hours by 16000 flight hours of testing. By extended fatigue testing an optional safe life requirement of 8000 flh could be reached.

Every 4000 flight hours of testing is followed by NDT-inspections of critical areas, using methods such as Eddy current, Fluorescent Magnetic particle and Penetrant, where applicable. Furthermore, the pretension of the bolts in the pylon to wing joint is also checked by a Raymond Bolt Gauge test.

The Pylon #4 fatigue test reached 16000 flight hours of testing without any cracks detected, verifying a safe life of 4000 flight hours. Due to a change in material of the bolts connecting the store mechanism to the pylon, the fatigue test was extended to 48000 flight hours of testing. No cracks were detected after 48000 flight hours of testing, thus also verifying the optional safe life requirement of 8000 flh. Later on, the Pylon #4 fatigue test object was reused in the previous described static test.

The fatigue test of Pylon #3 followed the Pylon #4 testing. At the moment the Pylon #3 has reached 12000 flight hours of testing without any cracks detected, and testing is continuing towards 16000 flight hours of testing.

Fatigue testing of Pylon #5 and Pylon #2 is scheduled to follow the Pylon #3 fatigue test.

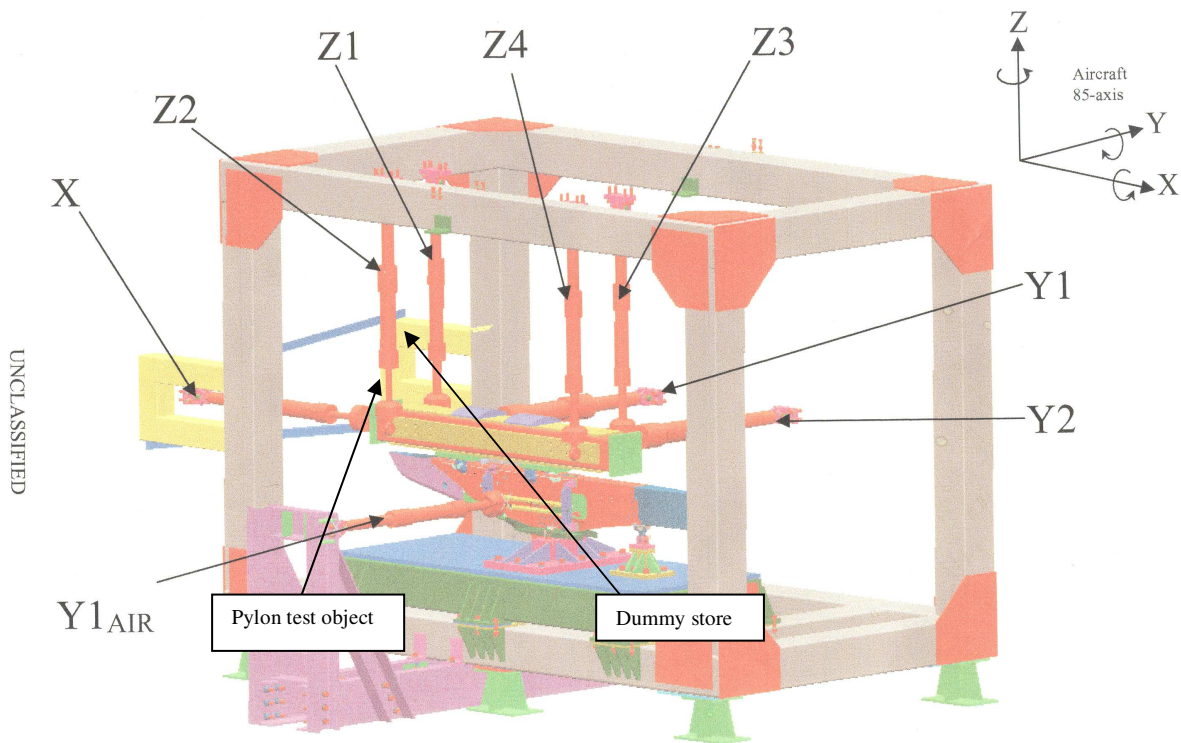


Figure 17. Export pylon static- and fatigue test rig.

3.3.9 Refuelling Transfer Units Fatigue Tests

Changed fatigue requirements on the aircraft refuelling equipments recently have been introduced on Gripen. An evaluation of historical qualification data therefore was considered necessary. For some units in the fuel system, a satisfactory result was not present in terms of verified fatigue strength. Based on equipment designs and existing qualification data package, a set of short term actions have been closed for the Forward and the Aft Refuelling Transfer Units (FRTU and ARTU):

- Load statistics from the Swedish Air-Force.
- Design load sequences for the units.
- Strain measurements and/or stress analyses on the units.
- Residual strength and/or fatigue testing of the units, illustrated by the ARTU test rig in Figure 18.
- Inspection programme on pre-flight aircrafts, illustrated in Figure 19 via detected cracks on an ARTU.
- Assessment of fatigue cracks and fracture surfaces with respect to reliability in NDT-inspection (Eddy Current and Penetrant).

The following main results with respect to fatigue are defined based on performed short term actions:

- The risk for fatigue cracks on the ARTU within specified aircraft service life can not be ignored regardless of aircraft versions. The level of risk however is affected by the aircraft version. Stable fatigue crack growth and damage tolerance, has been demonstrated by fatigue and residual strength testing.
- Structural areas with limitations in fatigue strength have been identified by stress analyses, fatigue testing and inspection programmes. Test rig results harmonize with in-service experiences.
- A Technical Sheet on local and focused NDT-inspection has been specified for the ARTU. Significant mechanical residual stresses in compression are present at the reinforcement ribs run-outs (Figure 18).

Based on above short term study, the following main consequences of changed fatigue requirement can be identified for the current production standards:

- Improved quality controls on the ARTU manufacturing process are required, illustrated in Figure 20 via a detected crack before entrance into service.
- Scheduled inspections (NDT) on the ARTU are required in order to maintain a safe structural function, illustrated by Figure 21.
- Maintenance actions on the transfer units within specified aircraft service life are required in order to maintain a safe structural function, replacement of selected screws.
- Limitation on the types of refueler in order to reduce pressure peaks at refuelling.

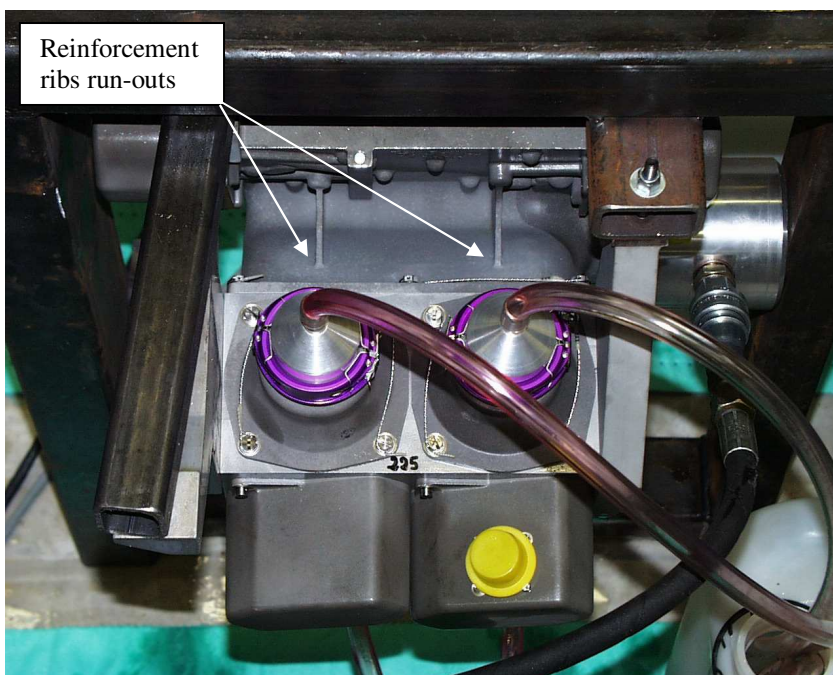


Figure 18. ARTU test rig - Fatigue and residual strength testing.

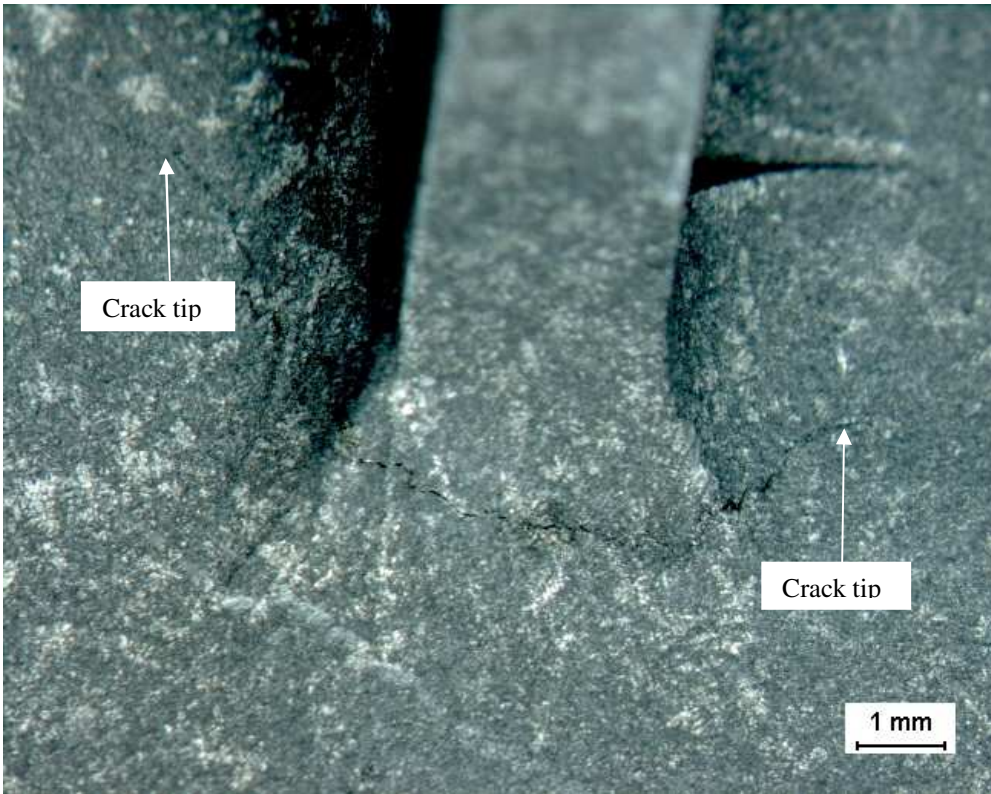


Figure 19. ARTU 1021 – Inspection results from an operational used unit. The crack is situated at one of the two reinforcement ribs on the manifold.

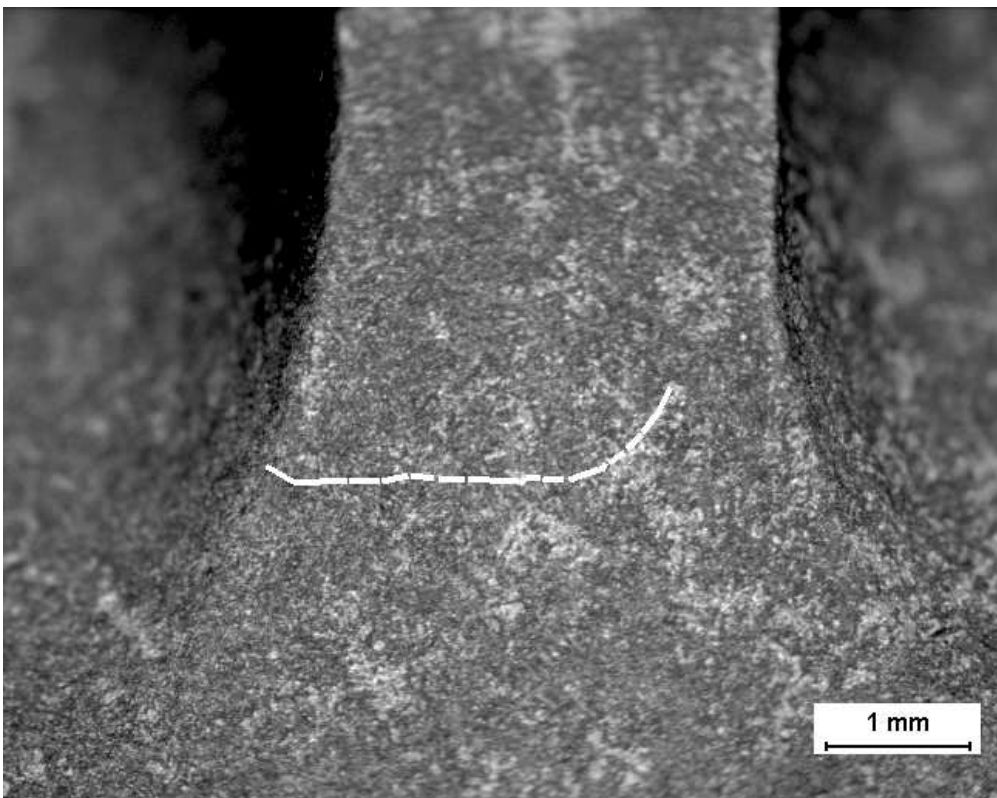


Figure 20. ARTU 1172 - The profile is based on SEM-examination and appearance after the tight crack was broken open. The crack is about 1.9 mm deep and about 3-4 mm long (surface).

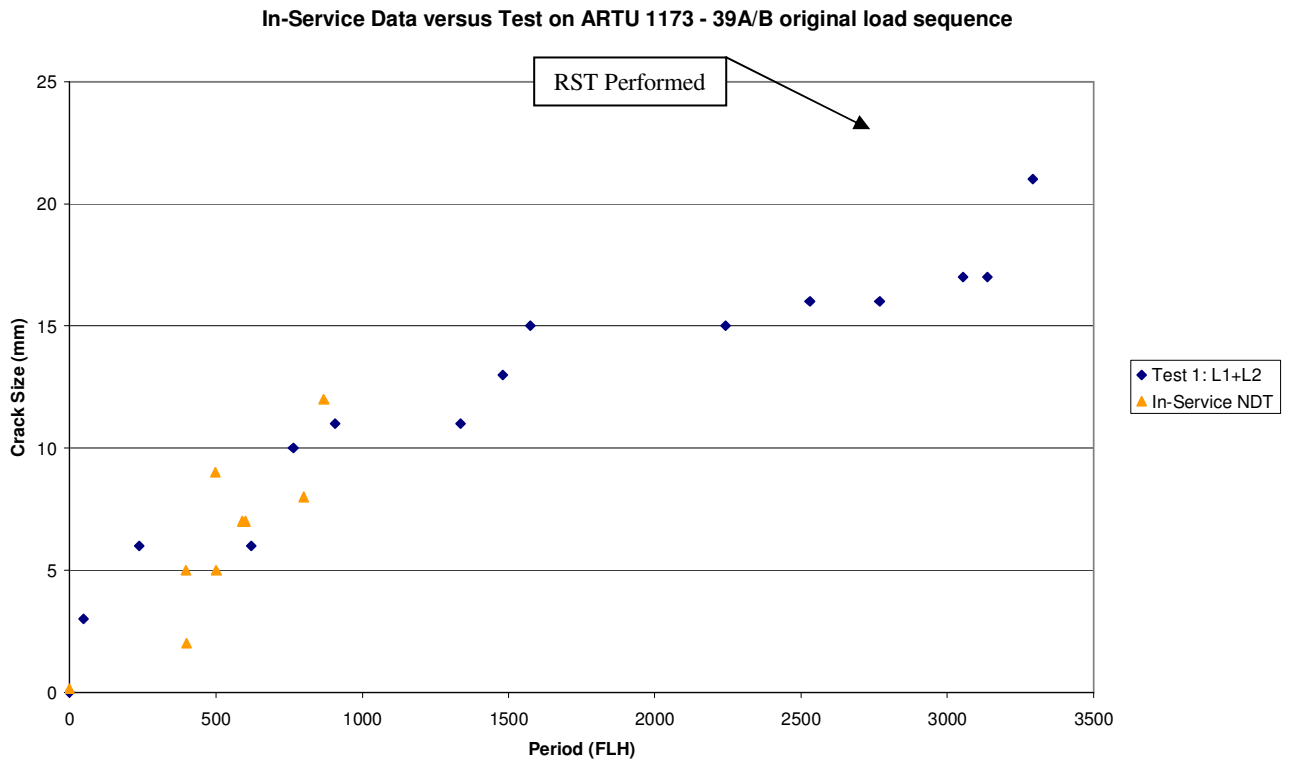


Figure 21. Crack size versus number of flight hour (severe refuelling only). The crack size reflected is the fatigue damage at one of the two reinforcement ribs. The in-service data are inspection results from eight cracked items but the test data are inspection results from one item (the initiation phase has been removed for the test item).

3.4 FATIGUE CRACK INITIATION AND PROPAGATION

3.4.1 Crack growth simulation for stiffened panels

Nowadays, the aircraft industry tries to replace build-up structures with integral structures. The main goals are to reduce the manufacturing and maintenance costs and also to decrease the weight of certain parts of the aircraft. The fuselage panels are an example of the aircraft parts that could be redesigned by changing the build-up configuration to integral configuration. However for such a change, studies have to be done to understand the behaviour of these new structures, particularly in the behaviour of fatigue and fracture.

Firstly, we study two kinds of stiffened panels for the crack growth behaviour using the finite element method (FEM). One example is shown in figure 22. Once this work is done, certain parameters (mesh, crack front shape) during crack growth are studied, see Figures 23 and 24. The final objective is to find the best model to simulate crack growth with FEM compared to experimental data.

To achieve these objectives, two stiffened panels are considered. The first one will be used to highlight the behaviour of the crack growth and to visualize the effects of the mesh and the crack front shape. The second study with a reference panel consists of using experimental data in order to find the best configuration to simulate crack growth in stiffened panels using FEM.

After these different studies, we have identified the effect of a stringer on the crack growth, see figures 25 and 26. The delay effect appears in all the stiffened panels (figure 26). FEM could highlight this phenomenon but the accuracy of the simulation depends on several important factors. To obtain good simulation results, we would pay a close attention to the mesh size used and to the order of polynomials chosen for the stress analysis. A high moderate p-value, for instance 6, associates to a good mesh brings us satisfactory results, see the convergence shown in figure 27. To change the crack front shape is not very important in this kind of FEM. Paris law appears to be sufficient for the studies we've made, however it could be interesting to study the efficiency of crack growth laws for the stiffened panels.

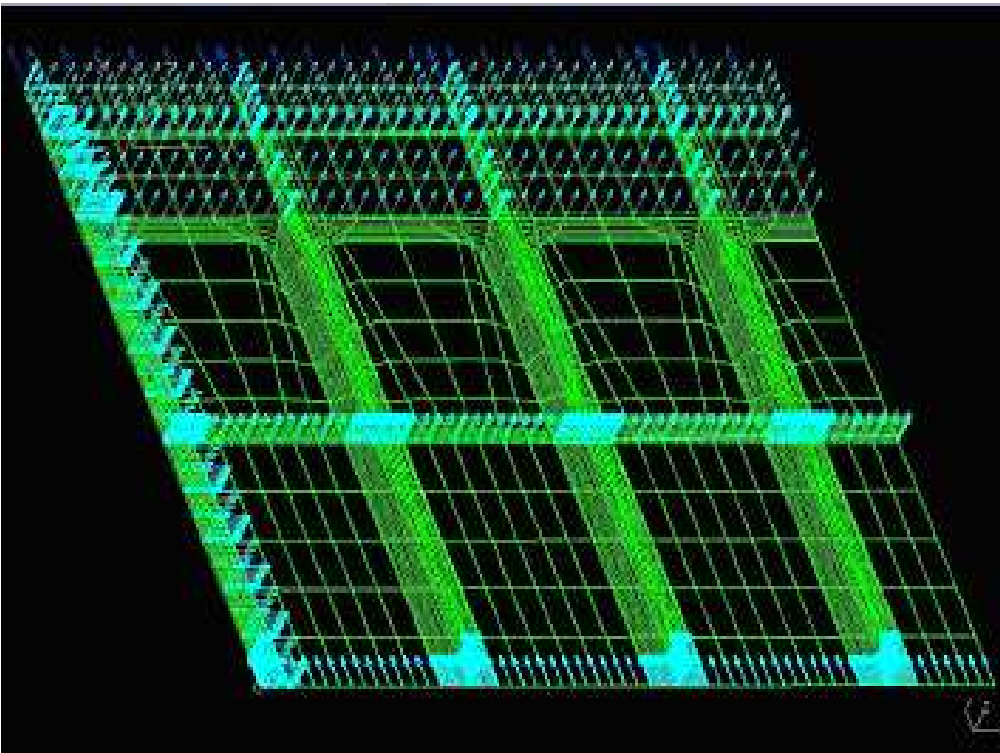


Figure 22. Reference panel boundary conditions

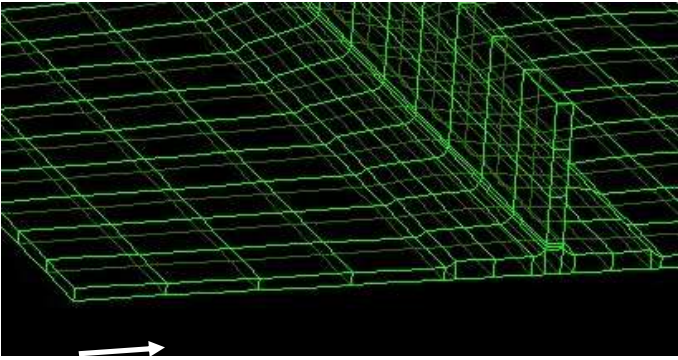


Figure 23. Localization and size of the crack

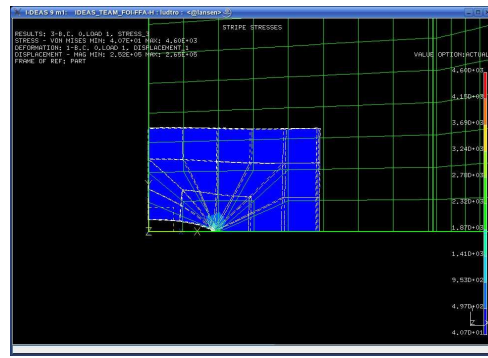


Figure 24. Mesh refinement for the stress intensity factor Computation

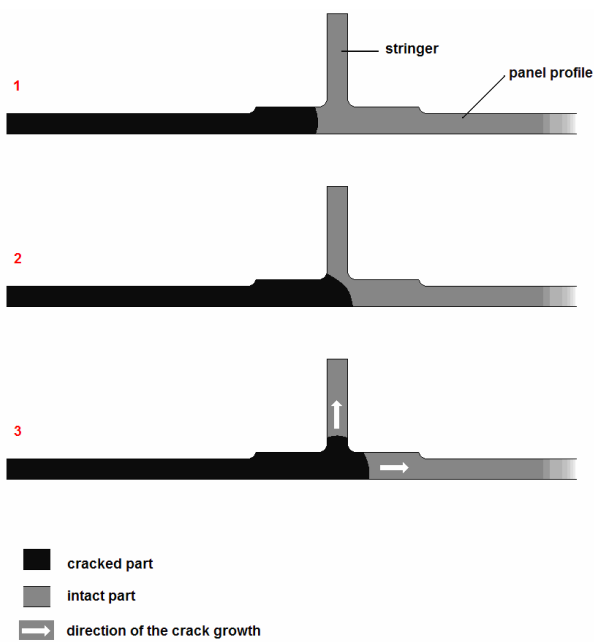


Figure 25. Fatigue crack branching

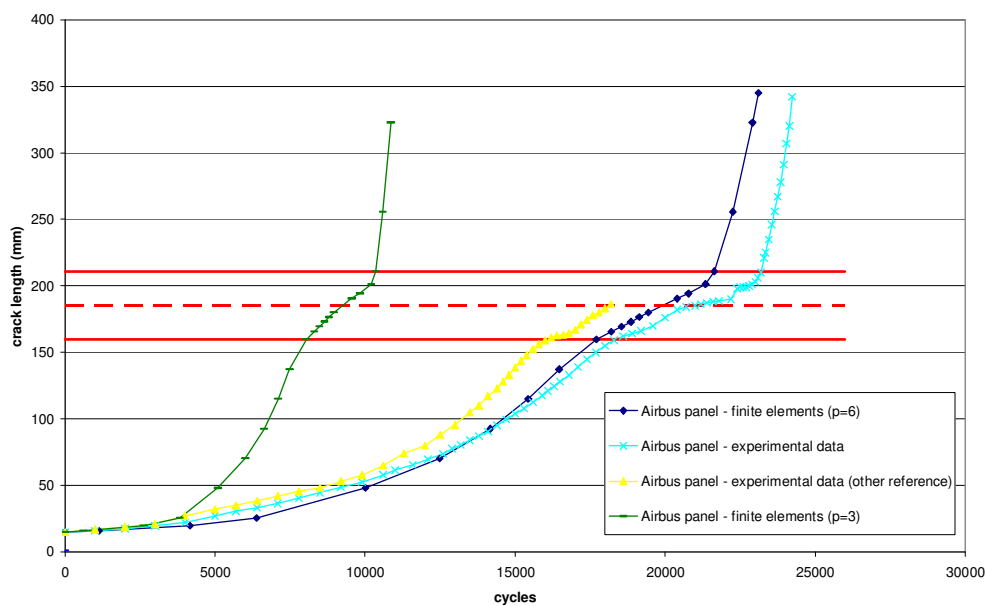


Figure 26. Effect of p -values on fatigue crack growth simulation results.

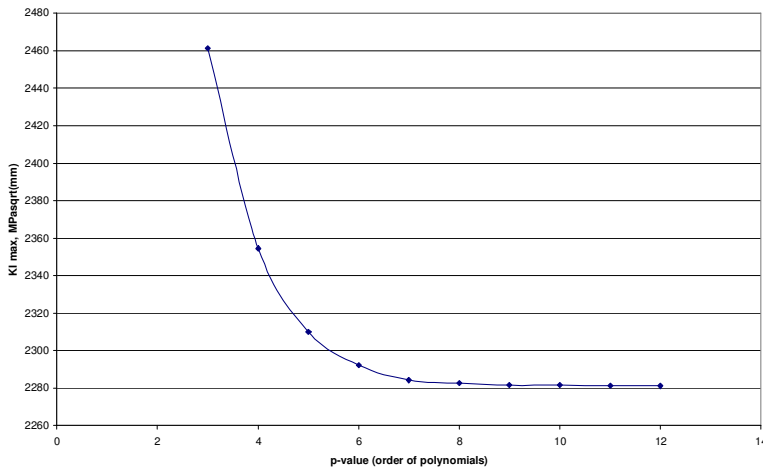


Figure 27. Convergence of the SIF with p -values

Reference

Ludovic Troncy, “Crack Growth Simulation for Stiffened Panels”, Technical Report FOI-R-2098-SE Oct. 2006, Stockholm, Sweden

3.4.2 Stochastic evaluations of fatigue crack initiation and propagation

Stochastic fatigue crack growth analyses have been performed using the experimental fatigue crack growth data obtained for the cracks initiated from metallurgical inclusions at the notch of the specimen, the AGARD short crack growth experimental data, see figure 28. This investigation is not intended to analyse the feature of short crack growth, but to analyse the effect of the inclusion distribution on the time the crack is observed to be initiated, and the consequent stochastic fatigue crack growth behaviour to the break through fatigue life of the crack. The incremental stochastic crack growth analysis based on the fast Fourier transformation (FFT) and Monte Carlo simulation has been made according to a two step stochastic fatigue crack growth model which assumes that the fatigue crack growth consists of a rapid and slow pulse process. The fatigue crack growth is simulated from an initial flaw size, which is the inclusion size, to a large crack size.

The distribution of inclusions in the crack initiation direction used in the crack growth analysis is based on the electron scanning microscope inspection results. It represents the physical initial flaw in the analysis. The crack is assumed to be initiated from one location where the particle has its largest size on the surface of the notch. This initial flaw is then grown to the final size although multiple cracks are often observed in the experimental results. The assumption is acceptable since a criterion has been applied when collecting the experimental data to prevent crack interaction.

Along with the incremental FFT and Monte Carlo simulation, different closed form models have been analysed. Among them are Brownian closed form solutions with and without the initial flaw distribution, and a model based on the deterministic crack growth law and initial flaw distribution (similar to the USAF model but with different initial crack definition). These models represent different methods in state of the art of the probabilistic crack growth analysis methodology when the initial crack distribution is involved. The investigation is to evaluate sequence of simplification in the analysis of the crack initiated from a distribution of crack sizes.

Both the incremental simulation and the closed form solution agree reasonably well with the experimental results although the parameters used in the stochastic model are directly derived from the experimental data set for large crack, see figure 29. The investigation indicates that the scatter in fatigue life is mainly affected by the process of crack growth instead of the scatter in initial flaws so that the stochastic solution is indispensable for the present experimental results for which the final crack size is significantly larger than the initial flaw size. The stochastic solution combined with the effect of scatter in initial flaws is highly recommended although the stochastic solution with an average initial flaw size may provide surprisingly good results for the reliability analysis for the case when the initial flaw size is very small.

The model with a deterministic crack growth law and scatter in initial flaw seems to be unacceptable since they provide very nonconservative results in the probabilistic solution. Such model should be avoided in the reliability analysis of the crack growth problems unless the equivalent initial flaw size distribution according to the USAF reliability model is used instead of the physical initial flaw size distribution.

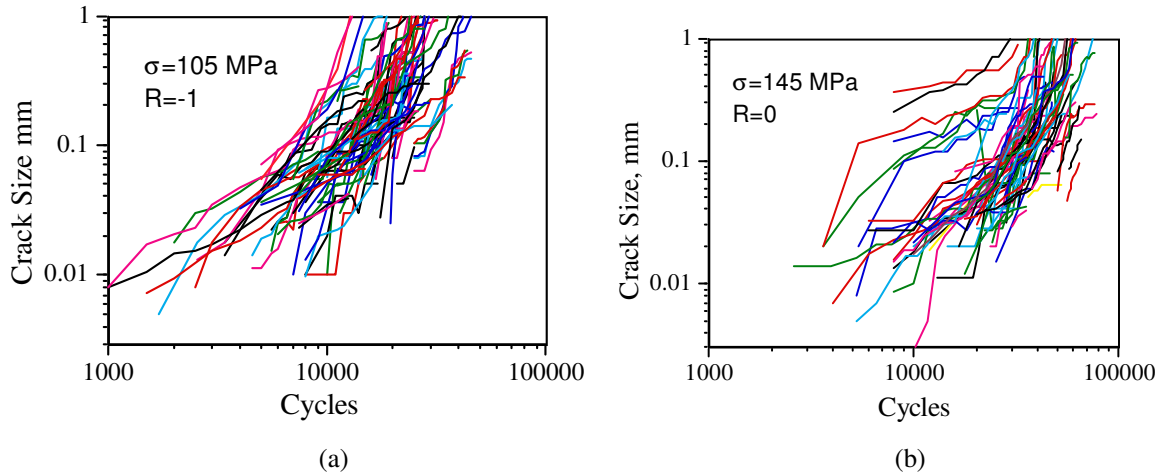


Figure 28. Experimental crack growth data for the surface crack length against number of cycles for the constant amplitude load of (a) stress ratio $R=-1$ and $\sigma_{max}=105$ MPa, and (b) $R=0$ and $\sigma_{max}=145$ MPa.

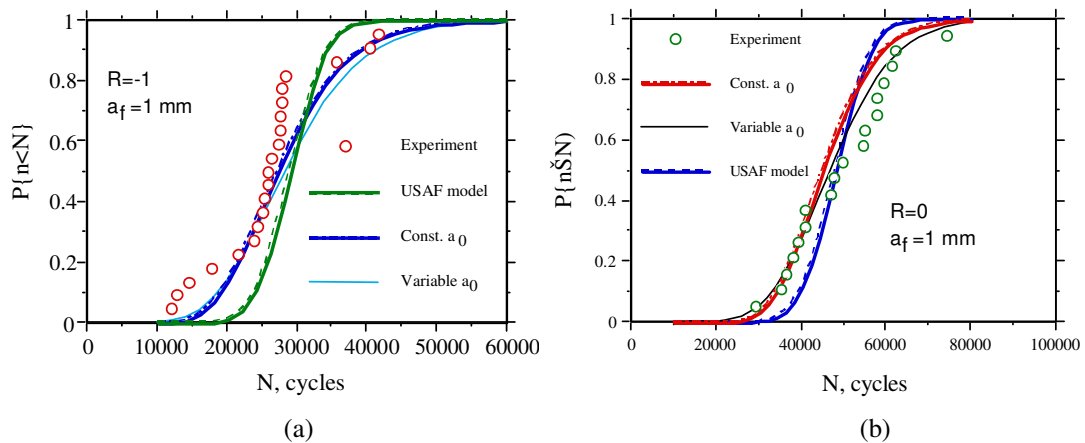


Figure 29. Comparison of the stochastic models with and without initial flaw distribution, the deterministic model with initial flaw distribution, and the experimental data for the probability of crack reaching the size of 1 mm for the stress ratio of (a) $R=-1$, and (b) $R=0$.

Reference

G. S. Wang, "Stochastic evaluations of fatigue crack initiation and propagation", The 16th European Conference on Fracture Mechanics: Failure Analysis of Nano and Engineering Materials and Structures, Greece, July 3-7, 2006

3.4.3 Towards large scale simulations of multiple site fatigue damages

It is a great challenge and of greatest importance to simulate fatigue crack initiation and propagation. Lack of basic understanding of basic physics in the process, effects of material properties, and difficulties in numerical solutions etc., often prevent a rational evaluation. Requirements for non-linear solutions like finite cyclic plastic deformation, contact and friction make things no easier even for the most advanced computational methods and computer platforms.

Fatigue damage depends on the quality of materials, constructions, loading, usage, and environmental effects. The process is highly stochastic. There is a great uncertainty in determining the probability of failure, especially when the construction is complicated and multiple cracks may be initiated. Full scale fatigue tests or the strip-down of ageing structures may give valuable information, but the cost is often prohibitive, and the obtained information is limited to

special cases. Analytical and computational methods, verified by some fatigue tests, are often the only resort to provide basic material and structural parameters for the life cycle safety and cost evaluations of new and ageing structures, see figure 30.

With the increased understanding of fatigue crack initiation and its propagation process at the complicated rivet joints, progress has been made towards the simulation of large aircraft structures with the help of modern computational capability and state of the art software engineering. With a global-local finite element solution, for example, thousands of fatigue cracks may be solved for the stress intensity factors of various crack sizes and configurations once the first solution for the crack-free structure is finished, see figure 31. This solution divides the numerical calculation into two steps; a global stress solution, and a local crack solution. Even with the computer capability available today that may deal with the finite element model having hundreds of thousands of degrees of freedom, it is still a great challenge for the fatigue crack evaluation. By dividing the problem further more into various sub solutions, the enormous computation capability may be fully exploited to simulate the fatigue crack growth process in a structure based on probabilistic methods like the Monte-Carlo and Markov chain models, with parameters obtained from coupon and substructure part fatigue tests, see figure 32.

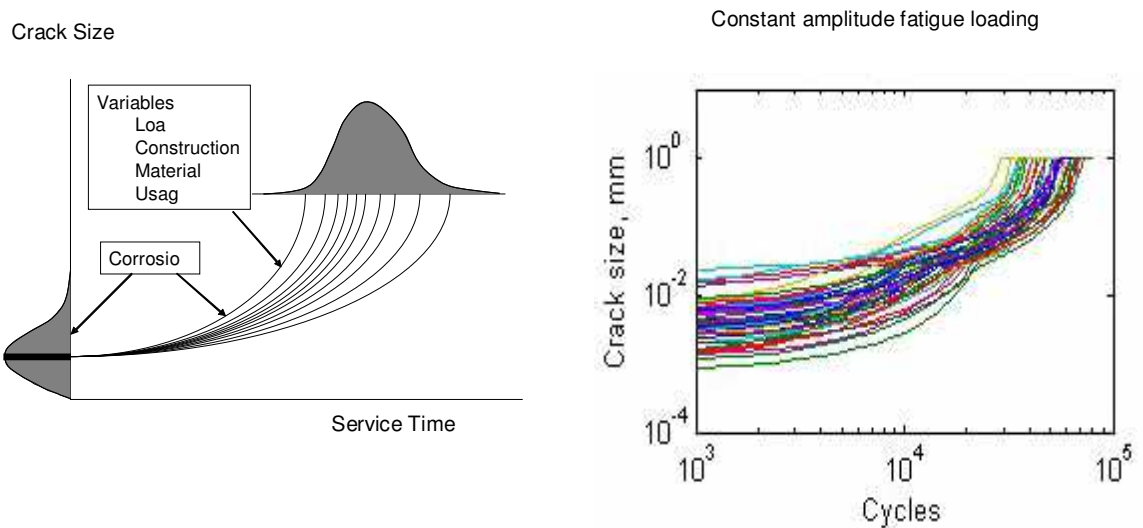


Figure 30. Stochastic fatigue crack initiation and propagation

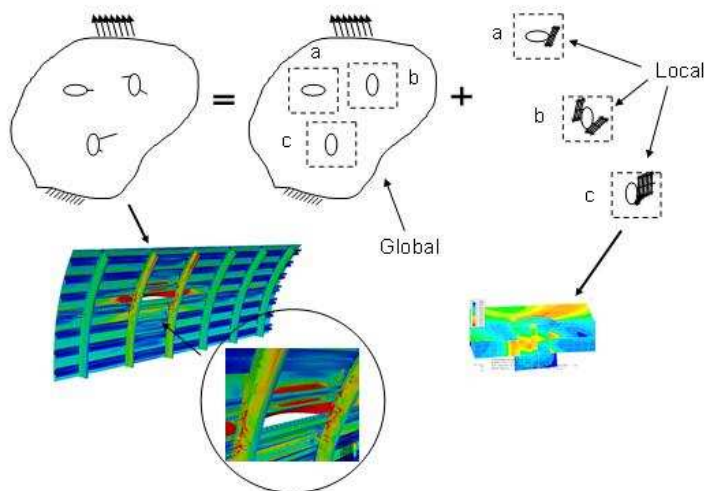


Figure 31. Schematic of global-local stress intensity factor solution.

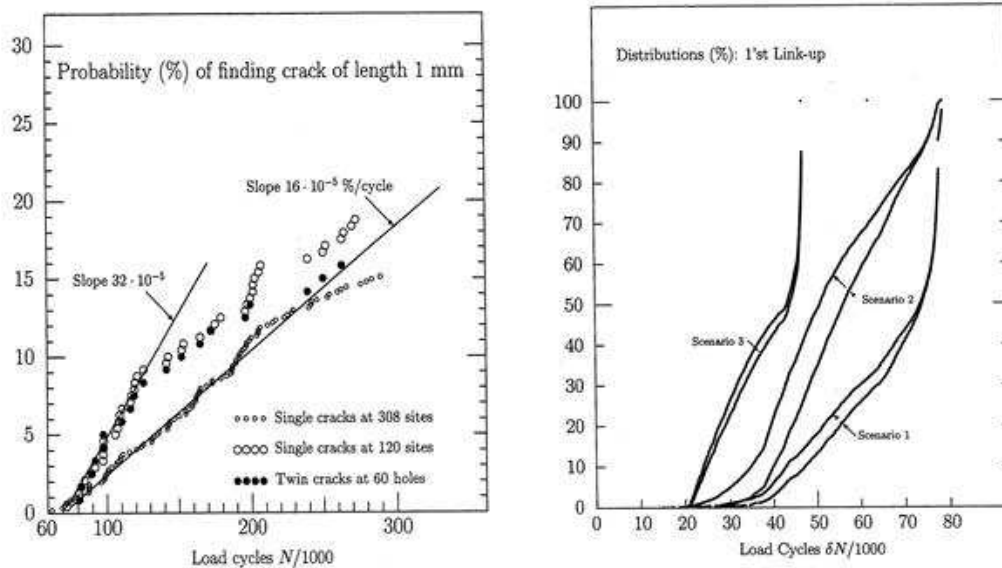


Figure 32. Monte-Carlo simulation of multiple crack link-up

Reference

G. S. Wang and A. F. Blom, "Towards large scale simulations of multiple site fatigue damages", Presentation at the 9th International Fatigue Congress, May 14-19, 2006, Atlanta, Georgia, U.S.A.

3.4.4 Crack propagation in welds

Most of the lifing of components are performed with crack initiation analyses. Some components are however considered to be critical for the aircraft safety and higher requirements apply. Such components can be engine mounts and flanges. Here VAC routinely carries out crack propagation analyses. Further, in the commercial engine industry loads followed by so called ultimate loads such as a fan blade off (where a fan blade separates from the shaft) with a large unbalance load as a result. If the engine stays on the wing the structure is to withstand the "wind milling" until the air craft can land safely. Also, during days of light weight design the capabilities of the material are being pushed further towards the limit thus the total life of the component may require additional life from crack propagation analyses. Some manufacturing procedures such as welding are yet being treated with special concern. Here a defect tolerance design method is employed.

The weld itself is treated as a part of the structure in terms of material properties. The special care to the weld is introduced when the local stress raisers due to offset and weld face and root reinforcement and radius between base material and the weld are taken into account. The current approach is to extract mean and bending stresses from a "master" stress FE-model (either shell or solid model) and calculate the local stress distribution from a sub-model.

Currently at collaboration between VAC and the Swedish Defense Research Agency a large number of crack propagation tests are underway. The test specimens have been manufactured for different weld classes with different offset levels and weld dimensions. A notch was introduced at the position where the stress peak is expected. The test

specimens will be exposed to a constant load ratio ($R > 0$) and the crack dimensions will be monitored during the test. A verification of analysis methods will be carried out at the end of the test program.

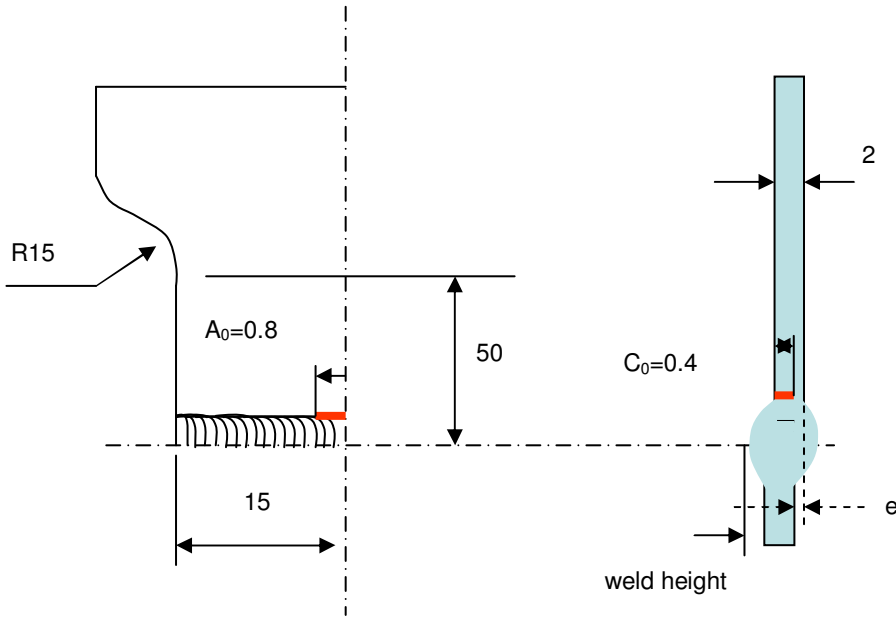


Figure 33. Test specimen

Sheet	Section	Class	Position	Drw offset (e)	Measured offset (e)	Weld height
Sheet 1	Snitt 1	Klass A	Topp	0	0	0.148
	Snitt 2	Klass A	Topp	0	0	0.189
	Snitt 3	Klass A	Topp	0	0	0.249
	Snitt 4	Klass A	Bot	0	0	0.409
	Snitt 5	Klass A	Bot	0	0	0.384
	Snitt 6	Klass A	Bot	0	0	0.42
Sheet 2	Snitt 1	Klass A	Topp	0	0	0.113
	Snitt 2	Klass A	Topp	0	0	0.302
	Snitt 3	Klass A	Topp	0	0	0.350
	Snitt 4	Klass A	Bot	0	0	0.468
	Snitt 5	Klass A	Bot	0	0	0.462
	Snitt 6	Klass A	Bot	0	0	0.462
Sheet 3	Snitt 1	Klass A	Topp	0.3	0.311	0.054
	Snitt 2	Klass A	Topp	0.3	0.383	0.113
	Snitt 3	Klass A	Topp	0.3	0.397	0.159
	Snitt 4	Klass A	Bot	0.3	0.381	0.228
	Snitt 5	Klass A	Bot	0.3	0.419	0.204
	Snitt 6	Klass A	Bot	0.3	0.418	0.165
Sheet 4	Snitt 1	Klass B	Topp	0	0	0.891
	Snitt 2	Klass B	Topp	0	0	1.09
	Snitt 3	Klass B	Topp	0	0	1.064
	Snitt 4	Klass B	Bot	0	0	0.584
	Snitt 5	Klass B	Bot	0	0	0.349
	Snitt 6	Klass B	Bot	0	0	0.474
Sheet 5	Snitt 1	Klass B	Topp	0.3	0.224	0.813
	Snitt 2	Klass B	Topp	0.3	0.112	0.991
	Snitt 3	Klass B	Topp	0.3	0.776	0.721
	Snitt 4	Klass B	Bot	0.3	0.456	0.387
	Snitt 5	Klass B	Bot	0.3	0.509	0.371
	Snitt 6	Klass B	Bot	0.3	0.339	0.576

Weld height will be machined. Specimens will be used for conventional CP-data testing

Measuring position / section 1-3 correspond to weld top-side
Measuring position / section 4-6 correspond to weld bot-side

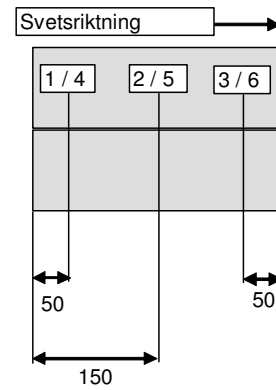


Figure 34. Test parameters

In design situations where a pre-fabricated design is chosen the structure will include a large number of welds and a fair amount of weld length (>20 m of weld). A fast method to calculate the crack propagation life in a weld is being developed using damage tolerance methods. The method is based on the following assumptions:

- Initial crack geometry is known (size and type)
- Thickness of the material is known and constant
- No load sequence effects
- No hold time effects on crack propagation rates included

An S-N table with calculated life can be produced and used to calculate the crack propagation life of the welds in the structure.

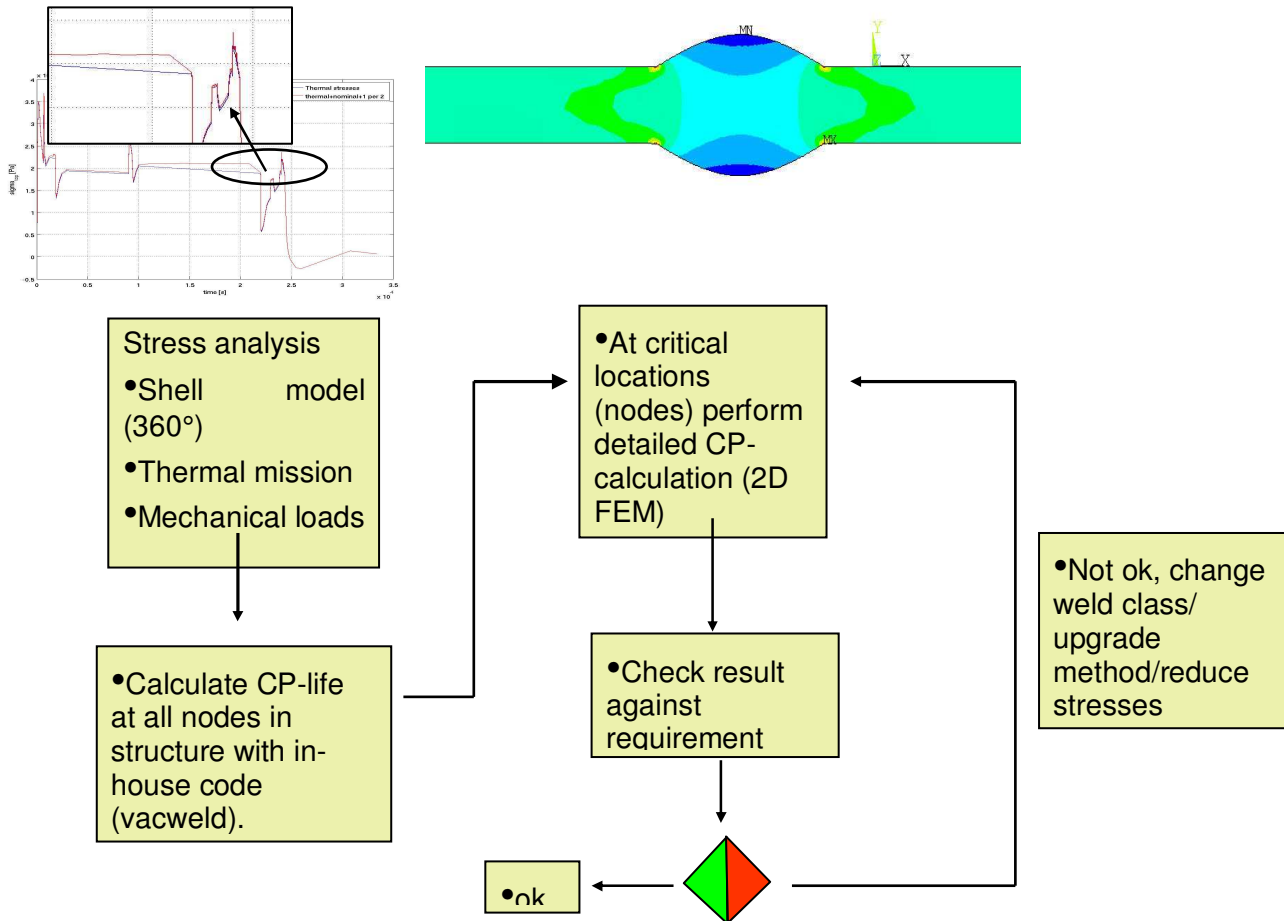


Figure 35. Design analysis procedure.

3.4.5 A modification to the Neuber rule

At fatigue life predictions, the analyst is often faced with the problem, that the stress-strain loading history is passing the yield limit of the material. A non-linear material model in the FE-analysis and a very long loading history is often not a realistic alternative. The yielding is therefore handled by some method for elastic-plastic correction. One such method is the Linear rule. Another is the universally accepted Neuber rule $\sigma \cdot \epsilon = \text{const.}$ At Volvo Aero we now suggest a modification to the Neuber rule.

The Neuber rule can be rewritten to
$$\sigma = \frac{\text{const.}}{\epsilon}.$$

Our modification, which we call the Super Neuber rule, can be written
$$\sigma = \frac{\text{const.}}{\epsilon^q}.$$

With this new format, it is with $q=\text{infinity}$ possible to identify the Linear rule, and with $q=1$ the Neuber rule. These possibilities to identify widespread methods for making elastic-plastic corrections of linear elastic stress and strain

results are of course pleasant, but not the main benefits of the new formulation. The main advantage is, that in contrast to the Linear rule and the Neuber rule, the new formulation allows for high quality elastic-plastic corrections. Such high quality elastic-plastic corrections are possible, if the loading can be characterized as proportional.

Best stress- and strain results are of course achieved if the FE-analysis of the complete loading sequence is performed with a suitable non-linear material model. As already made clear, this is often not practical, if at all possible.

A simple load cycle, consisting of for instance “start”-“maximum load”-“stop” should however most often be possible to perform with a suitable non-linear material model. Having such a result, it is now possible to perform a linear analysis on this same simple load cycle, and match q in $\sigma = \frac{const.}{\epsilon^q}$, so that best possible agreement between the non-

linear result and the corrected result is achieved. Now, if the loading is proportional, a high-quality elastic-plastic correction on the complete load sequence can be performed with this value of q . It must be noted that apart from being material dependent q is also geometry dependent and hence different for different nodes. This fact, and the procedure for matching q , intensifies the need of a computer program for the corrections. We have our own computer program, *elasplasgen*, to do the work. Today it simulates a kinematic hardening procedure, but it can be adapted also to isotropic hardening if necessary.

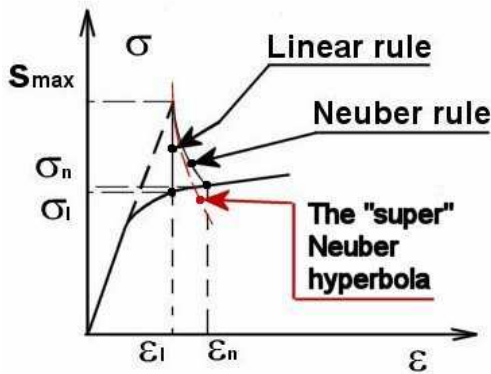


Figure 36. The super Neuber hyperbola.

3.4.6 Critical plane method for crack initiation analysis

At Volvo Aero crack initiation analysis is one important principle for fatigue life predictions. Most crack initiation analyses today are performed with so called one-parameter models: only one parameter (such as “maximum principal strain”) is extracted from, and representing, the often very complicated states of stress- and strain. During the last decades so called critical plan models have emerged, also called two-parameter models. Two parameters are extracted and represent the state of stress- and strain. With two parameters the ability to handle complicated situations, such as multiaxial states of stress and non-proportional loading, is supposed to increase.

After some considerations, we (Volvo Aero) have selected the Fatemi and Socie critical plane model as our main candidate for complimenting or replacing our one-parameter models. We have therefore in detail studied and further developed damage calculation and efficient methods for finding the critical plane. We have also studied methods for material data extraction and tested the performance of the Fatemi and Socie critical plane model on a number of “simpler” component tests. We have been able to show, that the Fatemi and Socie critical plane model works well and on a level with our one-parameter models for those “simple” cases of stress- and strain, which we so far have been limited to in our validation tests. A final step before the Fatemi and Socie critical plane model is adopted as a design tool, is to compare its predictions with validation tests containing high degree of multiaxiality and non-proportional loading.

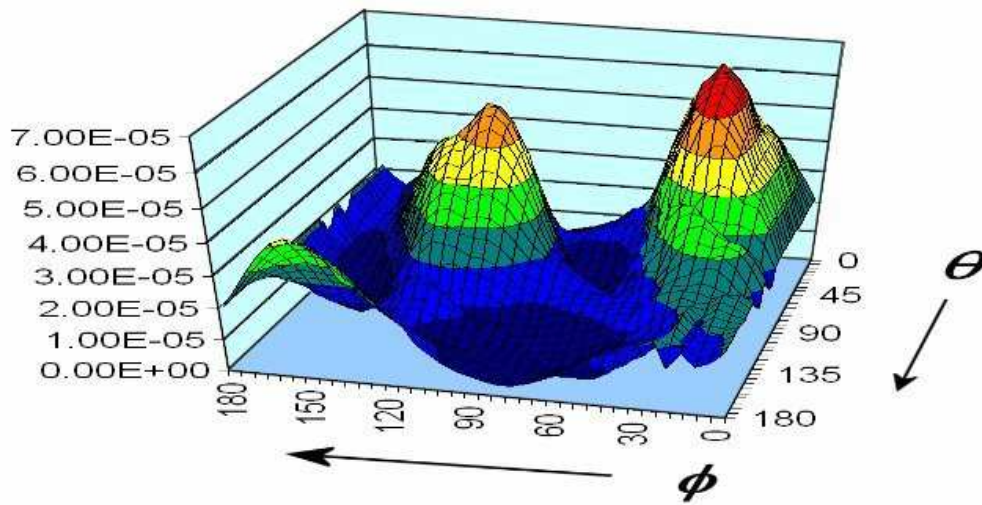


Figure 37. Damage versus plane orientation ϕ and θ

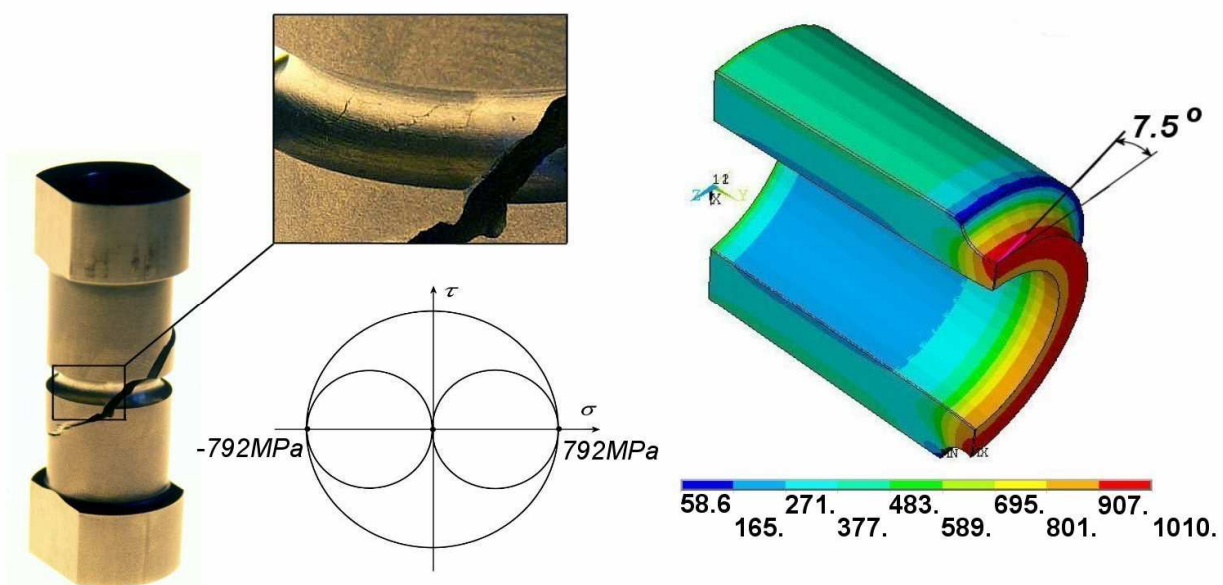


Figure 38. Component test torsion, stress distribution, critical plane orientation

3.4.7 Reliability based life prediction

A simple method for judging and taking into account variation and uncertainties in the fatigue analysis process has been developed in cooperation between Fraunhofer-Chalmers Research Centre of Industrial Mathematics and Volvo Aero. During the work focus has been on how to handle uncertainties and also to establish a method which is easy to use. The main purpose with the new method has been to establish a tool, which can be routinely used for calculating the reliability of a life prediction. Today this tool is used at the life management of the engine RM12 for JAS Gripen and it is considered as being one of the most important improvements in the fatigue analysis process at Volvo Aero during the last decade.

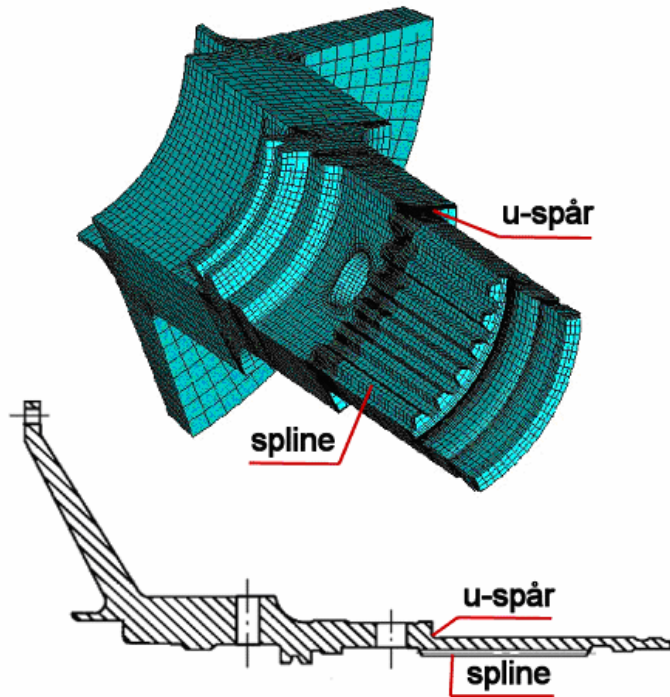


Figure 39. Analysis models, geometry etc.

Analysis models information + geometric tolerances information + material data information + load data information + component test data information + field experience information => "Easy-to-use" Reliability Tool. Results are given in terms of confidence intervals for predicted life taking all available data into account plus actual safety factor which should have been used if the design was performed with only nominal data.

3. Component tests performed, some service experience.

Data and models	Influence on crack initiation life		
	scatter τ	uncertainty δ	total
Mtdl data (ln is normal-) distr.			0.170
-pooled multiaxial-sequence effe 	0.170		
Material data, stat. uncertainties			0.138
-statistical uncertainty multiaxialit 		0.105	
-statistical uncertainty sequence		0.090	
Geometry			0.400
-tolerances 	0.400		
Model uncertainty			0.140
-Basquin-Coffin-Manson-model		0.050	
-mean stress influence		0.075	
-stress analysis, plasticity 		0.049	
-stress analysis, model quality		0.096	
-temperature effects		0	
-frequency influence		0	
Other uncertainties			0.133
- Flight/service loads 	-	0.133	
Total	0.435	0.237	0.495

		1780 (ges av -3sigma)
Urspr. pred.		4943
Pred. N		10602 4943 x 1.65x1.3
Pred. ln(N)	9.269	
95%	+2std(ln(N))	0.991
Pred.int. ln(N)	8.278	10.260
Pred.int N	3 936	28 554
99%	+2.58std(ln(N))	1.278
Pred.int. ln(N)	7.991	10.547
Pred.int N	2 953	38 059
99.8%	+3std(ln(N))	1.486
Pred.int. ln(N)	7.783	10.755
Pred.int N	2 399	46 861
	1780x0.75=	1335
Safety factor	(99.9%) S=	4.420

Figure 40. Analysis models information and results.

3.4.8 Fatigue testing of metal laminate coupons

A feasibility study of Metal Laminates has been undertaken by fatigue life testing of a number of combinations of metal sheet test coupons with a drilled hole for a number of different adhesives. The aim of the study is in brief to among other things to compare the fatigue life and evaluate if there is a combination of metallic material and adhesive that is superior to the others and if this is the fact try to understand why. The material chosen for the laminates was with a few exceptions based on clad material. When analysing the result one should not forget that the fatigue curves are based on just one specimen at each load level and also that the fatigue life range studied is far away from the fatigue limit. The results show the following. The unclad 2524 double and triple laminates show the longest fatigue life. The triple laminate of type 25-74-25 the second best and the double laminate of 2524 the third best. The rest of the laminates on the other hand turned out to be inferior to the others. Those were, triple laminate 74-25-74, double laminate 74-74 and 74-25.

The general improved fatigue behaviour of Metal Laminates compared to monolithic is based on a belief that crack initiates, stop at an interface, re-initiates in the second layer and so on. A similar effect caused by the laminate is the so called Crack divider effect locally reducing crack tip triaxiality. A possible consequence of this could be that a laminate with extremely good bonding is inferior to one with not so good bonding and so on.

The testing of the ML coupons in this project is based on an assumption that cracks start to grow from a drilled hole and then propagate through the sheet until final fracture. The residual stress state after drilling is an important factor for crack initiation. In this study the clad layer is another possible site for crack initiation.

The fact that two triple layer laminates are superior to the two layered ones in this study is not the main cause since there is another triple laminate that is not. What the two high fatigue life laminates have in common is also the fact that one of the components is unclad material while the other triple laminate is not. The biggest difference in life between the ML is mainly to be referred to early crack initiation caused by the clad layer of the material.

Having tested four different types of adhesives in this study the role of the adhesive has to be discussed. Since it is very difficult to find any difference in fatigue life between the four different types of adhesive used one could rather conclude that the behaviour is more like it had been with only one type of adhesive. This could be used in the discussion to argue that if the influence of the adhesive is ignored up to four specimens have been tested at each load level. This is very interesting since the observed quality varied a lot between the adhesives. The film adhesive showed very little pores while the paste adhesive showed gigantic pores. The question still remains whether the quality of the adhesive is at all critical for the uniaxial tension-tension fatigue properties or not. The answer is probably no or even that "bad quality" adhesive could improve the fatigue life properties.

In order to compare the two materials all data for the double laminates 2524 and 7574 have been put together neglecting the influence of adhesive type to evaluate their fatigue properties and plotted in figure 41. The difference in fatigue properties is more pronounced at lower life and the reason why the curves come together at higher life could be explained in the following way if the tests had been based on more than one specimen at each load level. It is generally found that the ratio between the life spent during crack initiation and the total fatigue life is high close to the fatigue limit. This would indicate that the differences caused by the metal laminate design could be found in the upper part of the curve. In order to investigate the influence of the clad layer a test was run using bare specimens in monolithic and as metal laminates together with a triple laminate from an earlier study figure 42. In summary the specific properties connected to a metal laminate are based on the possibility to take advantage of the delay and re-initiation of a crack. In this case cracks are initiated very easily in a clad layer which is a clear disadvantage in this case. The other aspect based on the change from plain strain to plain stress condition in the laminate is also a questionable mechanism for increased fatigue unless the reference has a much thicker cross section. The ideal material would then be a multilayered ML composed of outer clad sheet for design reasons inner layers of sheet with an optimal combination of crack initiation resistance and crack growth properties. This will need further testing focused on evaluation of the influence of the factors mentioned above.

A feasibility study of the properties of Metal Laminates has been undertaken. The study has mainly been concerned with fatigue testing of coupons and the following conclusions can be made.

- Unclad material in combination with clad material is superior to the others
- Double 2524ML is better than double 7475ML at low fatigue life.
- The cladding of the sheet is reducing the fatigue properties of ML
- Residual stress is a possible positive factor for unclad ML

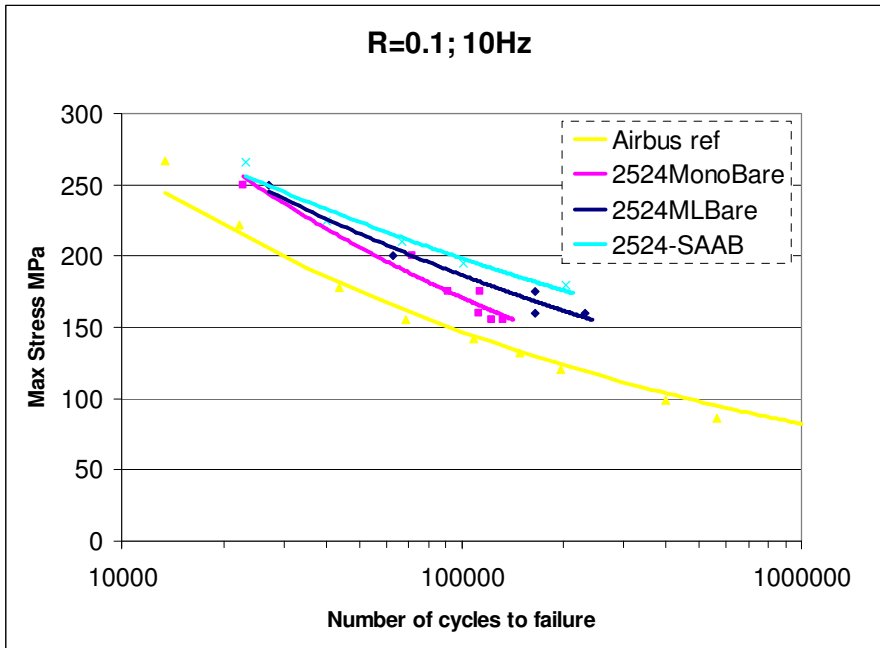


Figure 41. Fatigue curve showing a comparison between al clad double laminates in 2524, 2024, 74-25-74 and monolithic 2024 as reference (Airbus ref) plotting all adhesive types on one curve with power law fit of data

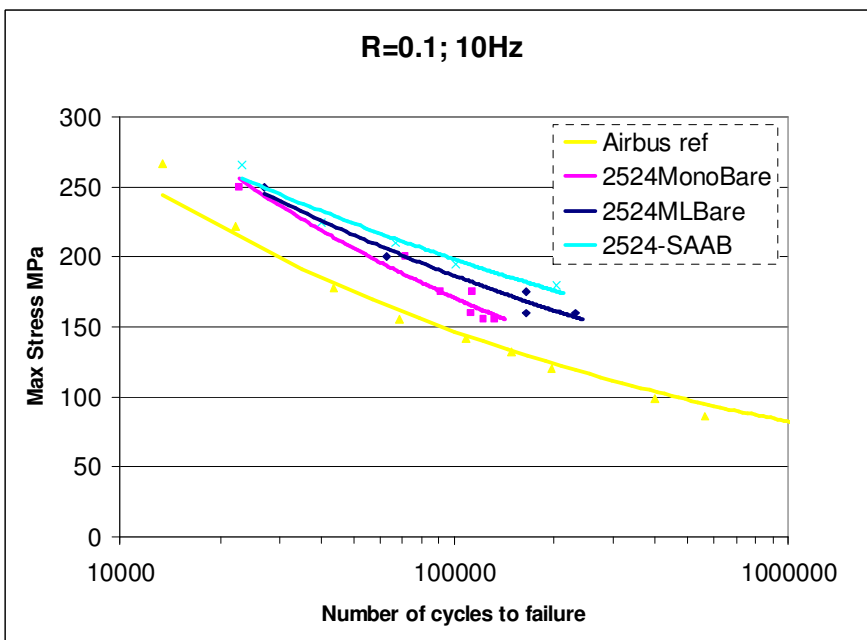


Figure 42. Fatigue curve showing a comparison between specimens of bare material in monolithic and as Metal Laminate (ML) (2524 MLBare and 2524-SAAB) compared to monolithic clad 2024 (Airbus ref)

3.5 COMPOSITE MATERIALS

3.5.1 Delamination fatigue modelling and constant mode fatigue behaviour

The well-known Paris law is the most commonly used method to model fatigue crack growth. In its simplest form, the Paris law can be written as:

$$\frac{da}{dN} = C(\Delta G)^r \quad (1)$$

where da/dN is the propagation rate of the delamination, a is the delamination length, N is the number of cycles, ΔG is the total energy release rate range, and C and r are propagation parameters which must be determined experimentally. In this expression, ΔG does not take into account the individual contribution of the different modes. In the literature, see ref [1] for details, other empirical expressions of the same law can be found, where the relative contributions of mode I and mode II are considered. In these models the mode mix dependence of the propagation parameters is only based on the propagation parameters for mode I and mode II. The variation of the parameters between the extreme values is made by an empirical function of the mode mix. In all these models the dependence is monotonic.

Results from fatigue delamination tests carried out under constant mode I (DCB - double cantilever beam test), mode II (ENF - end-notch flexure test) and 50/50 mixed modes I and II (MMB - mixed-mode bending test) are presented in Figure 43. Fitted lines for the three mode mixes taken into account are also included in the figure. For clarity, the values of the energy release rate range for each mode on the horizontal axis have been normalised by the critical energy release rate for each mode.

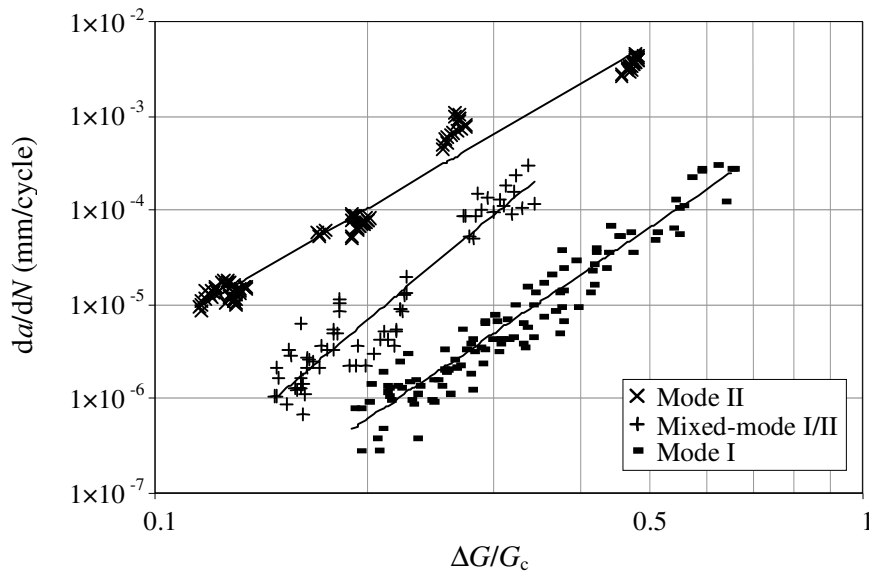


Figure 43. Experimental fatigue propagation rates for HTA/6376C

Despite the change in the horizontal axis, the differences between the three fitted lines are obvious. In the figure, it can be seen that the slope (the exponent r of the Paris law) for the case of the mode mix I/II is steeper than it is for mode I and mode II, which are relatively similar. It can be also seen that the intercept on the y axis (the coefficient C of the Paris law) for the mode mix I/II case does not lie in between the other two. Thus, the values of the parameters C and r for the mode mix I/II test do not lie in between the corresponding values for mode I and mode II, as is expected for a monotonic variation. Figures 44 and 45 show the experimental propagation parameters C and r , respectively, for the HTA/6376C carbon-epoxy laminate according to equation (1) as a function of the mode mix. The figures also include the 95% confidence bounds for the experimental propagation parameters. The best fit for the models found in the literature are also included. In the figures, a non-monotonic function is also included so that a comparison can be made. This model is proposed as a consequence of the results of the present investigation, and the details are presented in the next section.

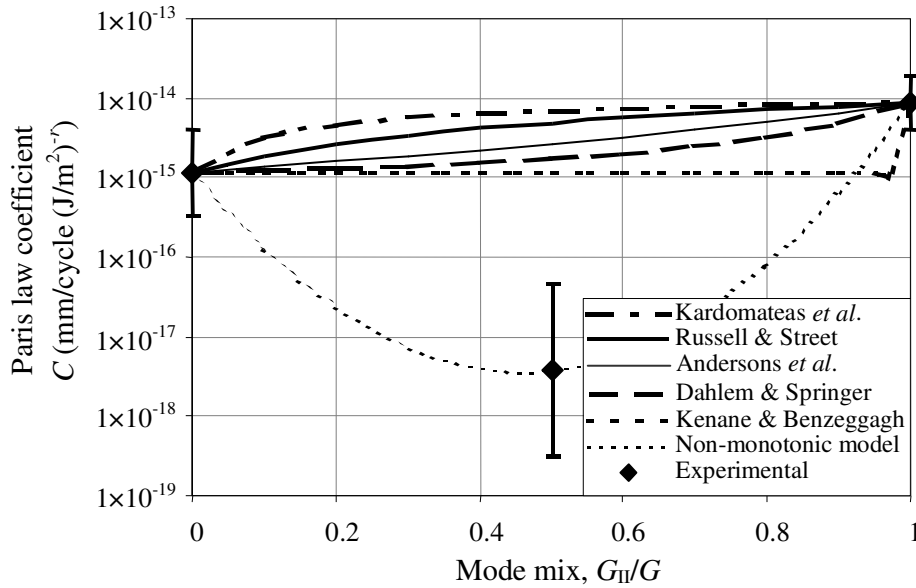


Figure 44. Comparison of the evolution of the crack propagation coefficient between the models from the literature and the experimental values of HTA/6376C

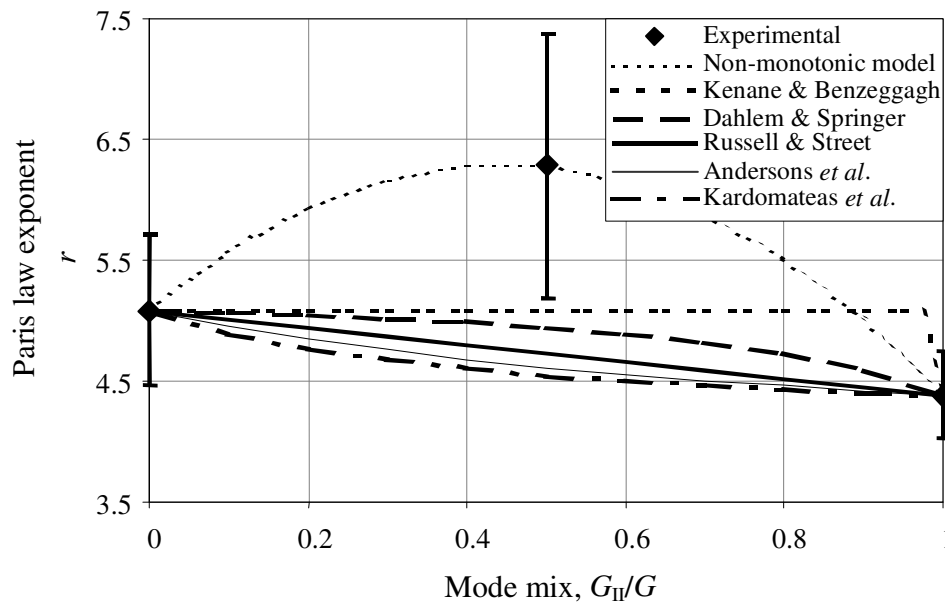


Figure 45. Comparison of the evolution of the crack propagation exponent between the models from the literature and the experimental values of HTA/6376C

A comparison of the shape of the different curves in Figures 44 and 45 shows that none of the models from the literature reviewed in [1] are able to capture the tendency of the propagation parameters when the mode mix I/II is included. All the models are monotonic and use the mode I and mode II experimental propagation parameters to describe their development with the mode mix in a monotonic way. None of the monotonic models from the literature are therefore able to predict the non-monotonic variation of the experimental propagation parameters with sufficient accuracy for this material. Hence, the formulation of a new non-monotonic model able to capture the real variation of the propagation parameters shown in the previous figures is justified.

Non-monotonic model

To describe the non-monotonic variation, generalized expressions, with experimentally adjusted factors, are justified. A set of parabolic equations is suggested to obtain the propagation parameters C and r . The expressions for both parameters are given by

$$\log C = c_1 + c_2 \left(\frac{G_{II}}{G} \right) + c_3 \left(\frac{G_{II}}{G} \right)^2 \quad (2)$$

$$r = r_1 + r_2 \left(\frac{G_{II}}{G} \right) + r_3 \left(\frac{G_{II}}{G} \right)^2 \quad (3)$$

The ratio of the mode II energy release rate to the total energy release rate is used as a measure of the mode mix. Analogous to expressions (2) and (3), a parabolic function depending on the ratio G_{II}/G can be formulated. The expression proposed here can be seen as a modification of the mixed-mode failure criterion introduced by Yan *et al.* [3], namely:

$$G_c = g_1 + g_2 \left(\frac{G_{II}}{G} \right) + g_3 \left(\frac{G_{II}}{G} \right)^2 \quad (4)$$

With these basic relationships an expression of the Paris-law is introduced, where the non-monotonic variation of the parameters is taken into account. The proposed expression is given by

$$\frac{da}{dN} = D \left(\frac{\Delta G}{G_c} \right)^r \quad (5)$$

where the parameters D , r and G_c depend on the mode mix G_{II}/G according to equations (2)-(4). The coefficient is now denoted by D to discriminate between the two Paris law expressions (1) and (5); D always has the unit length per load cycle, whereas the unit for C depends on the value of the exponent r .

Fatigue delamination growth under variable mode mix

A series of tests was carried out to characterize the delamination growth at different mixed modes under fatigue conditions for a unidirectional HTA/6376 composite. Crack propagation tests with a slightly varying degree of mode mix were carried out with a mixed-mode end-loaded split (MMELS) test. This test is similar to the mode II end load split (ELS) test where the external load is only applied to one of the cantilever beams of the specimen. A sliding clamp end is used to avoid normal axial forces as the specimen bends. Figure 46 represents, schematically, the test set-up for the MMELS test.

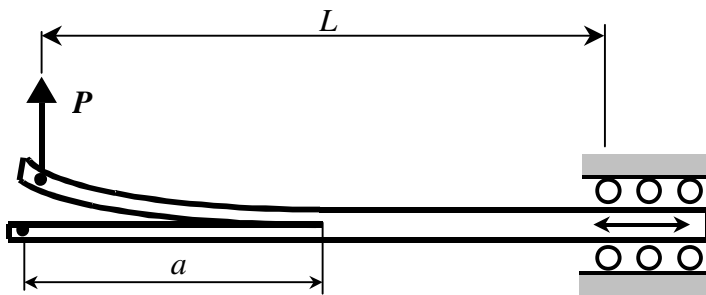


Figure 46. Mixed-mode end-loaded split test

The variation of the mode mix in the MMELS test can be calculated as a function of the delamination length. The variation of the mode mix for the specimens tested in the MMELS test is shown in Figure 47.

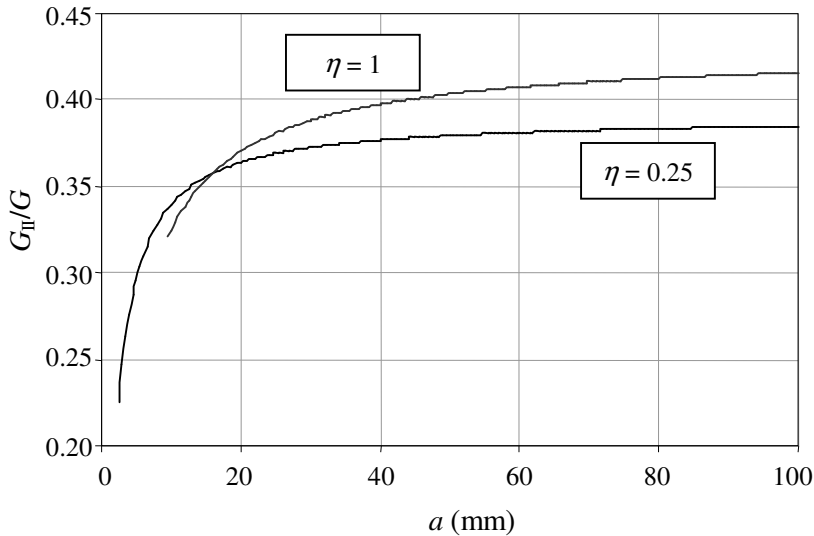


Figure 47. Mode mix variation for the MMELS specimens according to Bao et al. [4], η is the ratio between the thickness of the loaded and unloaded beams of the specimen.

Results and validation of non-monotonic model

Due to the unstable behaviour of the MMELS test, especially for short delamination lengths, the applied load levels had to be manually readjusted to maintain a subcritical progressive delamination growth and avoid the propagation of the delamination under static conditions, [1, 2]. However, only some of the results from the fatigue tests could be analysed. The scatter in the propagation behaviour of the fatigue-tested specimens was large. Figure 48 shows the evolution of the delamination length versus the number of cycles for one tested specimen of each type, $\eta = 0.25$ and $\eta = 1$.

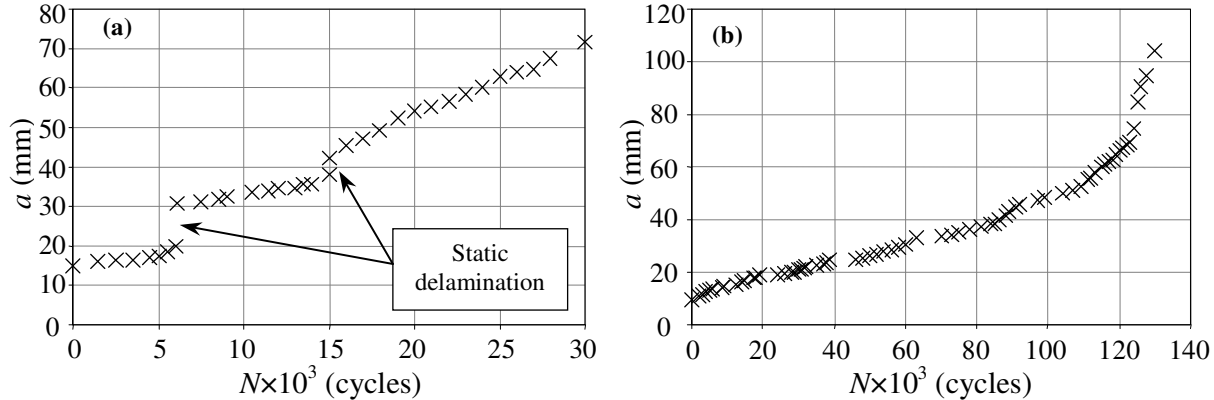


Figure 48. Crack length versus number of cycles for the MMELS test. (a) $\eta = 0.25$ specimen and (b) $\eta = 1$ specimen

During the propagation of the delamination in a MMELS test, the mode mix is changing continuously; however, for sufficiently long cracks, the mode mix only varies slightly during crack propagation (as shown in Figure 47). In Figure 49, two Paris plots are presented based on the data in Figure 48, in which the mode mix did not vary to any considerable degree. The experimental results are compared to the predictions of the modified Paris law, equation (5), including the propagation parameters D and r predicted by the non-monotonic model.

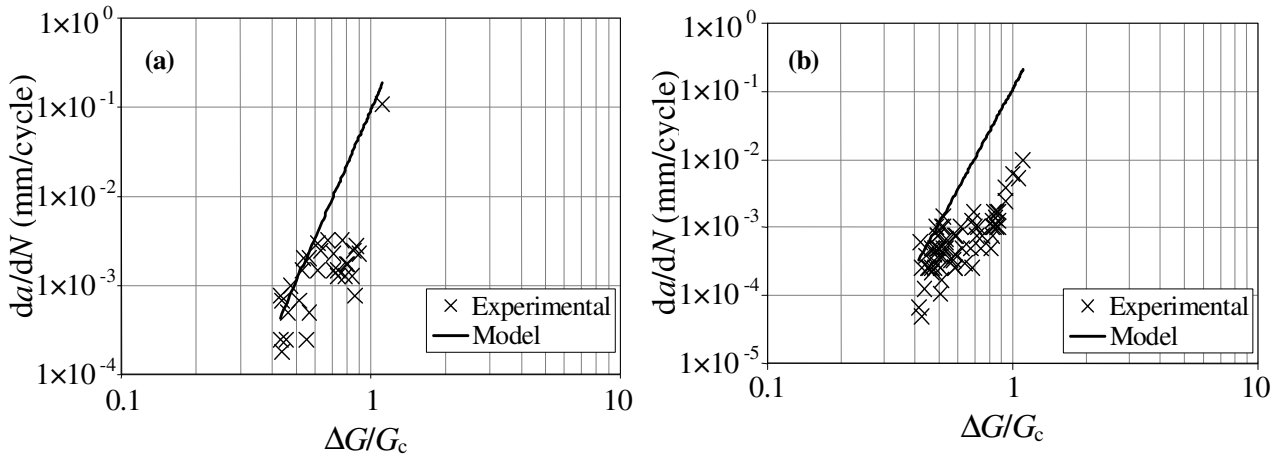


Figure 49. Crack propagation rate vs. normalised strain energy release rate for a MMELS test. (a) $\eta = 0.25$ specimen and (b) $\eta = 1$ specimen

It can be seen that the simulated propagation rate, based on experimental data in constant-mixed mode, overestimates the propagation rate in the MMELS test, and therefore serves as a conservative prediction. The scatter between specimens was quite large, especially during the growth of short cracks. Despite these imperfections, the proposed method for predicting crack growth from constant mixed-mode tests is a viable route towards predicting growth during more general conditions and with better accuracy than is the case with the monotonic models. A statistical approach would, however, be preferable since the variability in data is significant.

Conclusions

The Paris law parameters of fatigue delamination growth in constant mode mix at different degrees of mode I and mode II have been shown to vary non-monotonically with the degree of mode mix. This is generally not taken into account in existing methodologies for growth rate predictions. A generalized model to account for this non-monotonic dependency on mode mix was presented, and applied to data from a mixed-mode end-loaded split test. The predictions show only a fair correspondence with the experimental results, although the predictions were conservative. The non-monotonic model more accurately fits the experimental growth data of intermediate mode mixes, compared with previous propagation models.

References

1. Blanco, N., Gamstedt, E.K., Asp, L.E., Costa, J., Mixed-mode fatigue delamination in composite laminates, *International Journal of Solids and Structures*, Vol. 41, No. 15, 2004, pp. 4219-4235.
2. Blanco, N., Gamstedt, E.K., Asp, L.E., Costa, J., Experimental analysis of variable mixed-mode fatigue delamination in a carbon fibre-epoxy laminate, COMPTEST 2006, Porto, Portugal, April 10-12, 2006.
3. Yan, X.Q., Du, S.Y., Wang, D., An engineering method of determining the delamination fracture toughness of composite laminates. *Engineering Fracture Mechanics* Vol. 39, No. 4, 1991, pp.623-627.
4. Bao, G., Ho, S., Suo, Z., Fan, B., The role of material orthotropy in fracture specimens for composites, *International Journal of Solids and Structures*, Vol. 29, No. 9, 1992, pp.1105-1116.

ACKNOWLEDGEMENTS

This work was supported by Saab Aerosystems. The editor is also indebted to the following individuals who helped to write parts of this review:

Leif Asp	SICOMP	(Sections: 3.5.1)
Henrik Elinder	SHK	(Sections: 3.2.1)
Thomas Johansson	SAAB	(Section: 3.3.9)
Sten Johansson	LIU	(Sections: 3.4.8)
Tomas Månsson	VAC	(Sections: 3.4.4)
Leif Samuelsson	VAC	(Sections: 3.4.5, 3.4.6, 3.4.7)
Stefan Thuresson	SAAB	(Sections: 3.3.1, 3.3.2, 3.3.3, 3.3.4)
Geng-Sheng Wang	FOI	(Sections: 3.4.1, 3.4.2, 3.4.3)
Urban Wendt	SAAB	(Section: 3.3.8)